ON THE RELATION BETWEEN INFINITESIMAL SHAPE RESPONSE CURVES AND PHASE-AMPLITUDE REDUCTION FOR SINGLE AND COUPLED LIMIT-CYCLE OSCILLATORS

MAX KREIDER[1] AND PETER J. THOMAS[1−4]
CASE WESTERN RESERVE UNIVERSITY
[1]DEPARTMENT OF MATHEMATICS, APPLIED MATHEMATICS, AND STATISTICS
[2]DEPARTMENT OF BIOLOGY
[3]DEPARTMENT OF DATA AND COMPUTER SCIENCE
[4]DEPARTMENT OF ELECTRICAL, CONTROL AND SYSTEMS ENGINEERING

Abstract Phase reduction is a well-established method to study weakly driven and weakly perturbed oscillators. Traditional phase-reduction approaches characterize the perturbed system dynamics solely in terms of the timing of the oscillations. In the case of large perturbations, the introduction of amplitude (isostable) coordinates improves the accuracy of the phase description by providing a sense of distance from the underlying limit cycle. Importantly, phase-amplitude coordinates allow for the study of both the timing and shape of system oscillations. A parallel tool is the infinitesimal shape response curve (iSRC), a variational method that characterizes the shape change of a limit-cycle oscillator under sustained perturbation. Despite the importance of oscillation amplitude in a wide range of physical systems, systematic studies on the shape change of oscillations remain scarce. Both phase-amplitude coordinates and the iSRC represent methods to analyze oscillation shape change, yet a relationship between the two has not been previously explored. In this work, we establish the iSRC and phase-amplitude coordinates as complementary tools to study oscillation amplitude. We extend existing iSRC theory and specify conditions under which a general class of systems can be analyzed by the joint iSRC phase-amplitude approach. We show that the iSRC takes on a dramatically simple form in phase-amplitude coordinates, and directly relate the phase and isostable response curves to the iSRC. We apply our theory to weakly perturbed single oscillators, and to study the synchronization and entrainment of coupled oscillators.

keywords: isostable coordinates, entrainment, synchronization, limit cycle, shape-response curve, phase-response curve

AMS subject classifications: 34C20, 37N25, 92B25

1. Introduction.

Oscillations in physical systems are ubiquitous. Examples include flashing fireflies [64], spiking neurons [16, 23, 63], circadian rhythms [2, 17, 25], chemical reactions [29, 65], and rhythmic movement and locomotion [36, 56, 69]. Such oscillations can be modeled as non-linear dynamical systems with stable limit-cycle solutions.

The method of phase-reduction has been used extensively to study stable limit-cycle oscillations by characterizing the dynamics solely in terms of the *timing* of the oscillations [5, 16, 23, 32, 44]. The infinitesimal phase response curve (iPRC) is a useful tool for describing the change in timing of oscillatory dynamics under weak perturbation. Representing oscillators in terms of their phase facilitates analysis of the synchronization of weakly coupled oscillators, allowing one to predict the existence and stability of synchronous solutions, and to identify regions of mode-locking as a function of oscillator frequency [23]. Phase reduction has also been used successfully to study entrainment of oscillators subject to a weak external input, often in the context of a control problem [52, 78].

Traditional phase-reduction techniques are valid in the limit of weak perturbation, but tend to fail when system dynamics stray far from the unperturbed limit-cycle solution, such as in the case of large perturbations or large Floquet multipliers. Consequently, recent efforts have focused on introducing an extended framework that incorporates a sense of distance from the periodic orbit to augment a phase-like description. Concepts such as local orthogonal rectification [34], moving orthonormal coordinates [70], global phase (isochron) descriptions [13, 45], Koopman operator approaches [33], and isostable coordinates [7, 20, 73, 74, 75] have gained traction. The use of isostable coordinates is particularly convenient as it directly extends the phase description, leveraging Floquet theory to introduce amplitude (isostable) coordinates that obey linear dynamics. By considering an infinitesimal isostable response curve (iIRC), one can accurately predict the influence of weak perturbations on the "shape response" of the system, that is, the deformation of its orbit, allowing for a more accurate representation of system dynamics. Parallel techniques for studying oscillation amplitude include the homotopy analysis method [9, 35, 37, 41], nonlinear normal modes [54, 58, 59], harmonic balance methods [27, 30, 42], and the infinitesimal shape response curve (iSRC) [67, 77]. The iSRC, a variational approach that characterizes the shape response of limit-cycle dynamics subject to sustained perturbations, is especially suitable for studying weakly perturbed systems due to its ease of implementation and conceptual transparency. The iSRC gives an analytical expression for the shift in the *average* of any smooth function of the oscillator state; it has been used to provide a criterion for homeostasis in physiological systems based on oscillatory rather than fixed-point dynamics [77].

While different methods to analyze oscillator shape change are available, extensive literature in this area remains lacking despite the importance of oscillation amplitude in many physical systems. Circadian rhythm oscillations have traditionally been studied in terms of timing, focusing on sleep disorders, jet lag, and related issues. However, recent studies have linked changes in circadian rhythm amplitude to mental health disorders, obesity, increased risk of metabolic or cardiovascular disease, and conditions such as Alzheimer's or Parkinson's disease [1, 14, 24, 26, 62]. The oscillation of cytosolic Calcium plays a vital role in the regularization of cellular apoptosis; recently it was discovered that the amplitude, not the frequency, is the most relevant feature of the oscillations in this context [51]. Many mechanical systems display undesirable oscillations. Nonlinear aeroelastic systems can exhibit spurious oscillatory behavior, which results in system fatigue and decreased maneuverability [60, 61]. In downhole drilling systems, vibrations can lead to oscillatory phenomena and the premature failure of machine components [31]. In such situations, it is desirable to minimize the amplitude of the oscillations. A common approach is to establish a technique for estimating the amplitude, then subsequently apply a control strategy. Additionally, the amplitude of certain brain oscillations, such as theta-gamma waves, have been associated with memory and perception [12, 15].

To study the shape change of weakly perturbed and weakly driven oscillators, we leverage the existing techniques of phase-amplitude reduction and the iSRC, which have not been previously considered together. We establish phase-amplitude coordinates and the iSRC as complimentary approaches; for the first time, we connect the iSRC and phase-amplitude coordinates by expressing the iSRC in terms of the iPRC and iIRC of a system. We show that studying the iSRC in phase-amplitude coordinates is fruitful in that it provides intuition and a dramatically simplified conceptual approach to study the shape change of oscillations.

The paper is organized as follows. In section 2, we briefly review previously established results pertaining to phase-amplitude reduction and its numerical implementation, and the iSRC. Section 3 contains the main contributions of this work. We specify conditions for a general class of systems under which the iSRC may be expressed in phase-amplitude coordinates. In these cases, we show that the iSRC takes on a simple form. The iSRC is a vector equivalence class; we derive a novel expression that identifies the element of this class specified by an arbitrary choice of initial condition for the iSRC equation. We also derive expressions for higher order corrections to the iSRC. As a first application, we show how the complementary phase-amplitude iSRC approach may be used to study synchronization and entrainment of coupled oscillators. As a second application, we introduce an iSRC-based method to track the extrema of specific system states. This approach extends the limit-cycle homeostasis criterion [77] to give an expression for critical points (with respect to a perturbation parameter of state-variable extrema). In section 4, we apply our theory to several examples, including (non-planar) single oscillators under sustained perturbation, and the synchronization and entrainment of systems of coupled oscillators. We conclude in section 5 with a discussion of the results.

All codes used to generate the figures in this paper are publicly available at https://github.com/MaxKreider/PhaseAmplitudeISRC.git.

2. Background.

2.1. Phase-Amplitude Reduction.

In this section, we review the basics of phase-amplitude reduction. Consider an n-dimensional system

$$\mathbf{x}' = F(\mathbf{x};\epsilon) = f(\mathbf{x}) + \epsilon \cdot u(\mathbf{x}) \tag{2.1}$$

where $u(\mathbf{x})$ is a parametric perturbation and ϵ a small parameter characterizing the strength of the perturbation. Assume that when $\epsilon = 0$, (2.1) admits a T-periodic stable limit-cycle solution, $\gamma(t;0) = \gamma(t+T;0)$. One can define a phase variable $\theta(\mathbf{x}(t)) \in [0,T)$ on the limit cycle so that the phase evolves at a constant rate

$$\theta' = 1 \tag{2.2}$$

The notion of phase can be extended to the basin of attraction, Γ, of the limit cycle via isochrons [19, 76], or level sets of the phase function $\theta(\mathbf{x})$. If initial condition $\mathbf{x}_0$, with associated trajectory $\mathbf{x}(t)$, lies on the limit cycle with phase θ_0, then all initial conditions $\mathbf{y}_0 \in \Gamma$, giving rise to trajectories $\mathbf{y}(t)$, that satisfy

$$\lim_{t\to\infty} \|\mathbf{x}(t) - \mathbf{y}(t)\| = 0 \tag{2.3}$$

for any norm $\|\cdot\|$ are said to lie on the same isochron and have the same phase as $\mathbf{x}_0$. With this convention, the phase is defined in Γ and evolves at a constant rate. When $|\epsilon| \ll 1$, the phase dynamics obey

$$\theta' = 1 + \epsilon \cdot (Z_0(\theta))^T u(\mathbf{x}) + \mathcal{O}\left(\epsilon^2\right) \tag{2.4}$$

where $Z_0(\theta)$ is the infinitesimal phase response curve (iPRC) vector and represents the gradient of the phase function evaluated on the limit cycle. Eq. (2.4) is useful to study the change in timing of system oscillations due to a weak perturbation, but can fail to give an accurate representation of the dynamics in the case of strong perturbations. In such cases, one may define an additional $n-1$ amplitude (isostable) coordinates, σ_i, that capture a sense of distance in directions transverse to the limit cycle. The amplitude coordinates require concepts from Floquet theory, which we review in the supplementary materials in Appendix A, including the variational equation, the monodromy matrix, Floquet multipliers and exponents, and a non-resonance condition pertaining to the numerical implementation of phase-amplitude reduction.

2.1.1. Amplitude (Isostable) Coordinates. The additional $n-1$ amplitude coordinates are defined so that in the absence of perturbation, their dynamics admit a simple linear form

$$\theta' = 1, \quad \sigma' = \mathcal{K}\sigma, \quad \mathcal{K} = \mathrm{diag}(\kappa_2, \kappa_3, \ldots, \kappa_n) \tag{2.5}$$

where the κ_i are the non-trivial Floquet exponents of the system. One may find that a subset of the Floquet exponents are highly negative, meaning that the dynamics in the corresponding amplitude coordinates decay very rapidly to the limit cycle. In practice, one can disregard these directions, resulting in a system of reduced dimension with only $m \leq (n-1)$ relevant amplitude coordinates [43]. The perturbed ($\epsilon \neq 0$) system dynamics are expressed as

$$\begin{aligned} \theta' &= 1 + \epsilon \cdot (Z_0(\theta))^T u(\mathbf{x}) + \mathcal{O}(\epsilon^2) \\ \sigma_j' &= \kappa_j \sigma_j + \epsilon \cdot (I_0^{(j)}(\theta))^T u(\mathbf{x}) + \mathcal{O}(\epsilon^2), \quad j = 2, \ldots, m \end{aligned} \tag{2.6}$$

where $I_0^{(j)}$ are infinitesimal isostable response curves (iIRC), which are the gradients of the jth amplitude coordinate evaluated on the limit cycle. In practice, it is common to compute the response curves by finding the solution to the adjoint equations [7, 20, 23, 75]

$$\begin{aligned} \frac{dZ_0}{dt} &= -Df(\gamma(t))^T Z_0 \\ \frac{dI_0^{(j)}}{dt} &= -(Df(\gamma(t))^T - \kappa_j I_{n\times n}) I_0, \quad j = 2, \ldots, m \end{aligned} \tag{2.7}$$

with T-periodic boundary conditions and normalization constraints

$$\begin{aligned} (Z_0(0))^T f(\mathbf{x}_0) &= 1 \\ (I_0^{(j)}(0))^T v_j &= 1 \end{aligned} \tag{2.8}$$

where v_j is the eigenvector of the monodromy matrix corresponding to the jth Floquet exponent.

2.1.2. Numerical Implementation. The phase-amplitude framework (2.6) is an improvement over a purely phase-based description (2.4), but the resulting expansions are accurate to only first order in the amplitude variables. Recently, efforts have been made to compute higher order corrections, either by Taylor expansion methods [46, 72], or by the parameterization method [7, 20, 49]. While both theoretically give identical results, we use the parameterization method because we find it to be more accurate and computationally efficient. More precisely, if the following *phase-amplitude reduction assumptions* hold:

- (A1) The vector field $f(\mathbf{x})$ is analytic.
- (A2) System (2.1) admits a linearly asymptotically stable limit cycle, $\gamma(t; 0) = \gamma(t + T; 0)$, when $\epsilon = 0$.
- (A3) There does not exist a resonance at some order $|\alpha| = \alpha_2 + \cdots + \alpha_n \geq 2$ in the sense of definition SM1 (see supplementary materials, Appendix A).

then (2.1) admits a phase-amplitude reduction to arbitrarily high (finite) order

$$\begin{aligned} \theta' &= 1 + \epsilon \cdot (\mathbf{Z}(\theta, \sigma_2, \ldots, \sigma_m))^T u(\mathbf{x}) + \mathcal{O}(\epsilon^2) \\ \sigma_j' &= \kappa_j \sigma_j + \epsilon \cdot (\mathbf{I}^{(j)}(\theta, \sigma_2, \ldots, \sigma_m))^T u(\mathbf{x}) + \mathcal{O}(\epsilon^2), \quad j = 2, \ldots, m \\ \mathbf{x}(t) &= \mathbf{K}(\theta, \sigma_2, \ldots, \sigma_m) \end{aligned} \tag{2.9}$$

The function $\mathbf{K}(\theta, \sigma_2, \ldots, \sigma_m)$ should be thought of as a change of coordinates. The high order PRC and IRC functions, $\mathbf{Z}(\theta, \sigma_2, \ldots, \sigma_m)$ and $\mathbf{I}(\theta, \sigma_2, \ldots, \sigma_m)$, are expressed as Taylor expansions in terms of the amplitude coordinates. For example, if $m = 2$, one writes

$$
\begin{aligned}
\mathbf{Z}(\theta, \sigma_2) &= Z_0(\theta) + \sigma_2 Z_1(\theta) + \sigma_2^2 Z_2(\theta) + \ldots \\
\mathbf{I}^{(2)}(\theta, \sigma_2) &= I_0^{(2)}(\theta) + \sigma_2 I_1^{(2)}(\theta) + \sigma_2^2 I_2^{(2)}(\theta) + \ldots
\end{aligned}
\tag{2.10}
$$

where Z_0 and $I_0^{(2)}$ are the iPRC and iIRC functions, respectively.

We remark that if (A3) does not hold, one can still use the parameterization method, but will be unable to recover a linear field of the form (2.5) [49]. Further, note that there can be no resonance for $\alpha \in \mathbb{N}^n$ when [8]

$$
2 \le |\alpha| \le \frac{\mathrm{Re}(\mu_n)}{\mathrm{Re}(\mu_2)}
\tag{2.11}
$$

This fact implies that for any given system, there are only a finite number of possible resonances, the size of which is determined by the ratio of the real parts of the "largest" and "smallest" eigenvalues of R. Note that a two-dimensional system can never exhibit resonance in the sense of definition SM1. For a more detailed discussion of the resonance condition, the interested reader may consult [8].

The output of the parameterization method is not unique because the amplitude coordinates are defined up to an arbitrary multiplicative factor (see (2.8); any scalar multiple of an eigenvector is still an eigenvector). While any choice of normalization is equivalent mathematically, it is desirable to choose a normalization that, in practice, results in solutions which do not rapidly grow or decay. A precise description of the parameterization method, along with step-by-step instructions for its numerical implementation, may be found in [49].

2.2. infinitesimal Shape Response Curve. In this section, we briefly review iSRC theory. Consider a one parameter family of n-dimensional vector fields describing the dynamics of a single oscillator (coupled oscillators are analyzed later)

$$
\mathbf{x}' = F(\mathbf{x}; \epsilon) = f(\mathbf{x}) + \epsilon \cdot u(\mathbf{x})
\tag{2.12}
$$

with $u(\mathbf{x})$ a parametric perturbation of strength ϵ. If the following *single oscillator iSRC assumptions* hold: [67]

- (B1) There exists an open subset $\Omega \subset \mathbb{R}^n$ and an open neighborhood of zero $\mathcal{I} \subset \mathbb{R}$ such that the vector field $F(\mathbf{x}; \epsilon) : \Omega \times \mathcal{I} \to \mathbb{R}^n$ is $\mathcal{C}^1$ in both the coordinates $\mathbf{x} \in \Omega$, and the perturbation strength $\epsilon \in \mathcal{I}$.
- (B2) For $\epsilon \in \mathcal{I}$, system (2.12) admits a linearly asymptotically stable $T(\epsilon)$-periodic limit cycle, $\gamma(t; \epsilon) \in \Omega$, i.e., that $\{\gamma(t; \epsilon) \mid t \in [0, T)\} \in \Omega$.
- (B3) The limit cycle period $T(\epsilon)$ has $\mathcal{C}^1$ dependence on ϵ.

then (2.12) has a well-defined iSRC, $\gamma_1(t) = \gamma_1(t + T)$, satisfying

$$
\gamma_1'(t) = Df(\gamma(t; 0))\gamma_1(t) + \nu_1 f(\gamma(t; 0)) + \left.\frac{\partial F(\gamma(t; 0); \epsilon)}{\partial \epsilon}\right|_{\epsilon=0}, \quad \gamma_1(0) = \gamma_1(T) = p_1
\tag{2.13}
$$

with

$$
\nu_1 = -\frac{1}{T} \int_0^T (Z_0(s))^T \left.\frac{\partial F(\gamma(s; 0); \epsilon)}{\partial \epsilon}\right|_{\epsilon=0} ds
\tag{2.14}
$$

In (2.14), $T = T(0)$ is the unperturbed period of (2.12) and Z_0 is the iPRC.

The iSRC describes the shape response (deformation of the orbit) of a limit cycle under sustained perturbation to linear order in ϵ. That is, one writes

$$\gamma(\tau(t);\epsilon) = \gamma(t;0) + \epsilon\gamma_1(t) + \mathcal{O}(\epsilon^2), \quad \text{uniformly in } t \tag{2.15}$$

$$\tau(t) = t\left(1 - \epsilon\nu_1 + O(\epsilon^2)\right) \tag{2.16}$$

The scaled time, $\tau(t)$ (discussed in more detail in the proof of Lemma 3.2), permits a consistent comparison of the perturbed and unperturbed orbits at corresponding time points [67]. Eq. (2.13) can be understood in the following way. The first term is the variational equation describing the contraction of a small perturbation back to the stable limit cycle. The second term takes into account the shift in timing due to the perturbation, with ν_1 the change in frequency to linear order in ϵ. The third term represents a shape change (transverse expansion) due to the perturbation. Intuitively, the natural contraction of dynamics toward the limit cycle is exactly balanced by the transverse expansion due to the perturbation, resulting in a periodic solution.

The initial condition for (2.13), p_1, is chosen by fixing a Poincaré section, transverse to the unperturbed limit cycle at base point $p_0 = \mathbf{x}_0$, which intersects the perturbed limit cycle at point p_ϵ. One then chooses p_1 as the first order description of p_ϵ by writing

$$p_1 = \frac{p_\epsilon - p_0}{\epsilon} \tag{2.17}$$

The Poincaré section, Π, must be chosen transverse to $f(\mathbf{x}_0)$, but is otherwise arbitrary. Let $\mathcal{P}_{\vec{n}}^{(n-1)}(\mathbf{x}_0)$ be the space of smooth, simply connected $(n-1)$ dimensional surfaces transverse to $f(\mathbf{x}_0)$ with normal vector $\vec{n}$. Formally, we choose a section Π

$$\Pi \subset p \cap B_\eta^n(\mathbf{x}_0), \quad p \in \mathcal{P}_{\vec{n}}^{(n-1)}(\mathbf{x}_0) \tag{2.18}$$

where $B_\eta^n(\mathbf{x}_0)$ is the n-dimensional ball centered at $\mathbf{x}_0$ with radius $\eta > 0$, chosen so that Π does not intersect the unperturbed and perturbed orbits in more than one location. To eliminate ambiguity, we establish the convention that the sign of the normal vector, $\vec{n}$, is chosen so that $\vec{n} \cdot f(\mathbf{x}_0) > 0$. Different choices of section will result in different intersection points p_ϵ (and thus different initial conditions p_1), which in turn will result in different iSRCs. By Lemma 2.3 in [67], these iSRCs differ only by a fixed offset, which underlines an important fact: the iSRC is a vector equivalence class, whose elements are specific iSRCs determined by specific Poincaré section.

3. Results. We specify conditions under which a general class of systems is amenable to analysis via phase-amplitude reduction and the iSRC simultaneously.

THEOREM 3.1. *Consider a one parameter family of n-dimensional vector fields describing the dynamics of a single oscillator*

$$\mathbf{x}'(t;\epsilon) = F(\mathbf{x};\epsilon) = f(\mathbf{x}) + \epsilon \cdot u(\mathbf{x}) \tag{3.1}$$

subject to a parametric perturbation $u(\mathbf{x})$ with strength ϵ. Suppose that (3.1) satisfies the iSRC phase-amplitude assumptions

- *(C1) There exists an open subset $\Omega \subset \mathbb{R}^n$ and an open neighborhood of zero $\mathcal{I} \subset \mathbb{R}$ such that the vector field $F(\mathbf{x};\epsilon) : \Omega \times \mathcal{I} \to \mathbb{R}^n$ is analytic in the coordinates $\mathbf{x} \in \Omega$ and $\mathcal{C}^1$ in the perturbation $\epsilon \in \mathcal{I}$.*

- *(C2) For $\epsilon \in \mathcal{I}$, the system (3.1) admits a linearly asymptotically stable $T(\epsilon)$-periodic limit cycle $\gamma(t;\epsilon) \in \Omega$, where $T(\epsilon)$ has $\mathcal{C}^1$ dependence on ϵ.*
- *(C3) The non-resonance condition (A3) holds.*

Then, (3.1) admits a well-defined iSRC, $\gamma_1(t) = \gamma_1(t+T)$, with initial condition $\gamma_1(0) = p_1$ specified by a choice of Poincaré section transverse to $f(\mathbf{x}_0)$. Moreover, when expressed in phase-amplitude coordinates, the iSRC takes the form

(3.2)
$$\gamma_1(t) = \begin{bmatrix} 1 & & & \\ & \exp(\kappa_2 t) & & \\ & & \ddots & \\ & & & \exp(\kappa_n t) \end{bmatrix} p_1 + \begin{bmatrix} \int_0^t \Big(\nu_1 + Z_0(s)\cdot u(\gamma(s;0))\Big) ds \\ \int_0^t e^{\kappa_2(t-s)}\Big(I_0^{(2)}(s)\cdot u(\gamma(s;0))\Big) ds \\ \vdots \\ \int_0^t e^{\kappa_n(t-s)}\Big(I_0^{(n)}(s)\cdot u(\gamma(s;0))\Big) ds \end{bmatrix}$$

where the linear change in frequency, ν_1, is given by

$$\nu_1 = -\frac{1}{T}\int_0^T (Z_0(s))^T \frac{\partial F(\gamma(s;0);\epsilon)}{\partial \epsilon}\bigg|_{\epsilon=0} ds \tag{3.3}$$

Here, Z_0 and $I_0^{(j)}$ are the iPRC and iIRC of the unperturbed system (expressed in its original coordinates), the κ_j are the non-unitary Floquet exponents, and $T \equiv T(0)$.

For the sake of clarity, we give the proof of Theorem 3.1 in two steps. Lemma 3.2 shows that system (3.1) admits a well-defined iSRC. Lemma 3.3 shows that the iSRC can be expressed in phase-amplitude coordinates. A detailed discussion of the initial condition, p_1, is presented in the next section. Note that the iSRC phase-amplitude assumptions (C1-C3) represent a concise restatement of the single oscillator iSRC assumptions (B1-B3) and the phase-amplitude reduction assumptions (A1-A3) without overlap.

LEMMA 3.2. *Under assumptions (C1-C2), system (3.1) admits a well-defined iSRC, $\gamma_1(t) = \gamma_1(t+T)$, which satisfies*

$$\gamma_1'(t) = Df(\gamma(t;0))\gamma_1(t) + \nu_1 f(\gamma(t;0)) + \frac{\partial F(\gamma(t;0);\epsilon)}{\partial \epsilon}\bigg|_{\epsilon=0} \tag{3.4}$$

with linear shift in frequency, ν_1, given by

$$\nu_1 = -\frac{1}{T}\int_0^T (Z_0(s))^T \frac{\partial F(\gamma(s;0);\epsilon)}{\partial \epsilon}\bigg|_{\epsilon=0} ds \tag{3.5}$$

Proof. Define a new time variable $\tau(t) = \omega t$ for some $\omega(\epsilon) = \omega \in \mathbb{R}$ to be determined. Written as $\mathbf{x}(\tau(t);\epsilon)$, the solution of (3.1) obeys

$$\omega \frac{d\mathbf{x}}{d\tau} = \mathbf{F}(\mathbf{x},\epsilon) \tag{3.6}$$

Assumptions (C1-C2) guarantee a solution of the form

$$\begin{aligned} \mathbf{x}(\tau(t);\epsilon) &= \gamma(t;0) + \epsilon\gamma_1(t) + \mathcal{O}(\epsilon^2) \quad \text{(uniformly in } t) \\ \omega &= 1 + \epsilon\omega_1 + \mathcal{O}(\epsilon^2) \end{aligned} \tag{3.7}$$

Substitution of (3.7) into (3.6) gives, for the LHS

$$\begin{aligned}(3.8)\quad &\Big(1+\epsilon\omega_1+\mathcal{O}(\epsilon^2)\Big)\Big(\gamma'(t;0)+\epsilon\gamma_1'(t)+\mathcal{O}(\epsilon^2)\Big)\\ &\qquad=\gamma'(t;0)+\epsilon\gamma_1'(t)+\epsilon\omega_1\gamma'(t;0)+\mathcal{O}(\epsilon^2)\\ &\qquad=F(\gamma(t;0);0)+\epsilon\left[\gamma_1'(t)+\omega_1\gamma'(t;0)\right]+\mathcal{O}(\epsilon^2)\end{aligned}$$

and for the RHS

$$\begin{aligned}F(\mathbf{x};\epsilon)&=F\Big(\gamma(t;0)+\epsilon\gamma_1(t)+\mathcal{O}(\epsilon^2);\epsilon\Big)+\mathcal{O}(\epsilon^2)\\ &=F(\gamma(t;0);0)+\epsilon\frac{dF}{d\epsilon}(\gamma(t;0)+\epsilon\gamma_1(t)+\mathcal{O}(\epsilon^2);\epsilon)\Big|_{\epsilon=0}+\mathcal{O}(\epsilon^2)\\ &=F(\gamma(t;0);0)+\epsilon\left[\frac{\partial F}{\partial\mathbf{x}}\frac{d\mathbf{x}}{d\epsilon}+\frac{\partial F}{\partial\epsilon}\right](\gamma(t;0);\epsilon)\Big|_{\epsilon=0}+\mathcal{O}(\epsilon^2)\\ &=F(\gamma(t;0);0)+\epsilon\left[Df(\gamma(t;0))\gamma_1(t)+\frac{\partial F}{\partial\epsilon}(\gamma(t;0);\epsilon)\Big|_{\epsilon=0}\right]+\mathcal{O}(\epsilon^2)\end{aligned}\tag{3.9}$$

Equating the two expressions (noting that the $\mathcal{O}(\epsilon^0)$ terms match) and dropping higher order terms gives

$$\gamma_1'(t)-Df(\gamma(t;0))\gamma_1=-\omega_1 f(\gamma(t;0))+\frac{\partial F}{\partial\epsilon}(\gamma(t;0);\epsilon)\Big|_{\epsilon=0}\tag{3.10}$$

The Fredholm alternative establishes a solvability condition for (3.10). Note that the operator acting on $\gamma_1(t)$ is given by

$$L[\gamma_1(t)]=\left[\frac{d}{dt}-Df(\gamma(t;0))\right](\gamma_1(t))\tag{3.11}$$

along with T-periodic boundary conditions. The adjoint of L is

$$L^\dagger[\gamma_1(t)]=\left[-\frac{d}{dt}-(Df(\gamma(t;0)))^T\right](\gamma_1(t))\tag{3.12}$$

Note that the iPRC (up to normalization) spans the nullspace of $L^\dagger$. By the Fredholm alternative, a solvability condition for the existence of a T-periodic solution is

$$0=\int_0^T(Z_0(s))^T\left(-\omega_1 f(\gamma(s;0))+\frac{\partial F}{\partial\epsilon}(\gamma(s;0);\epsilon)\Big|_{\epsilon=0}\right)ds\tag{3.13}$$

Rearranging gives

$$\omega_1=\frac{\int_0^T(Z_0(s))^T\frac{\partial F}{\partial\epsilon}(\gamma(s;0);\epsilon)\Big|_{\epsilon=0}ds}{\int_0^T(Z_0(s))^T f(\gamma(s;0))ds}=-\frac{T_1}{T}=-\nu_1\tag{3.14}$$

where we used the normalization condition (2.8) pertaining to the iPRC function and where T_1 represents the linear shift in period [67]. As was to be shown, we conclude that the iSRC equation, along with appropriate initial condition, is given by

$$\gamma_1'(t) = Df(\gamma(t;0))\gamma_1(t) + \nu_1 f(\gamma(t;0)) + \frac{\partial F}{\partial \epsilon}(\gamma(t;0);\epsilon)\bigg|_{\epsilon=0} \tag{3.15}$$ ∎

The proof of Lemma 3.2 offers a derivation of the iSRC equation distinct from the original found in [67]. In [67] the re-scaling of time was imposed first, followed by the deformation of the orbit, without invoking the Fredholm alternative. Here, the shift in frequency falls out naturally from the solvability condition. Moreover, our derivation extends directly to treatment of coupled oscillators, as shown below. Our derivation follows an asymptotic analysis similar to that found in [28]. Lemma 3.3 to follow demonstrates that the iSRC equation admits a simple representation in phase-amplitude coordinates and completes the proof of Theorem 3.1.

Lemma 3.3. *Under assumptions (C1-C3), the iSRC of system (3.1) can be expressed in phase-amplitude coordinates*

$$\gamma_1(t) = \begin{bmatrix} 1 & & & \\ & \exp(\kappa_2 t) & & \\ & & \ddots & \\ & & & \exp(\kappa_n t) \end{bmatrix} p_1 + \begin{bmatrix} \int_0^t \Big(\nu_1 + Z_0(s)\cdot u(\gamma(s;0))\Big) ds \\ \int_0^t e^{\kappa_2(t-s)} \Big(I_0^{(2)}(s)\cdot u(\gamma(s;0))\Big) ds \\ \vdots \\ \int_0^t e^{\kappa_n(t-s)} \Big(I_0^{(n)}(s)\cdot u(\gamma(s;0))\Big) ds \end{bmatrix} \tag{3.16}$$

Proof. Assumptions (C1-C2) in conjunction with Lemma 3.2 show that (3.1) admits a well-defined iSRC. Under the additional assumption (C3), system (3.1) is guaranteed to admit a phase-amplitude reduction as described in §2.1.2. Recall that the phase-amplitude dynamics are given, to linear order in ϵ, by

$$\begin{aligned} \theta' &= 1 + \epsilon\cdot(\mathbf{Z}(\theta,\sigma_2,\dots,\sigma_n))^T u(\mathbf{x}) \\ \sigma_j' &= \kappa_j\sigma_j + \epsilon\cdot(\mathbf{I}^{(j)}(\theta,\sigma_2,\dots,\sigma_n))^T u(\mathbf{x}) \end{aligned} \tag{3.17}$$

In order to write the equations in terms of phase-amplitude coordinates alone, we substitute $\mathbf{x} = K(\theta,\sigma_2,\dots,\sigma_n)$, in the $u(\mathbf{x})$ terms. Expanding the K function in terms of the amplitude coordinates, we note that the zeroth order term is the unperturbed limit cycle [49]. Therefore, writing $\vec{\sigma} = [\sigma_2,\dots,\sigma_n]^T$, we have $\mathbf{x} = K(\theta,\vec{\sigma}) = \gamma(t;0) + \mathcal{O}(\|\vec{\sigma}\|)$. Consequently, the phase-amplitude dynamics go as

$$\begin{aligned} \theta' &= 1 + \epsilon\cdot(\mathbf{Z}(\theta,\vec{\sigma}))^T u(\gamma(t;0) + \mathcal{O}(\|\vec{\sigma}\|)) \\ \sigma_j' &= \kappa_j\sigma_j + \epsilon\cdot(\mathbf{I}^{(j)}(\theta,\vec{\sigma}))^T u(\gamma(t;0) + \mathcal{O}(\|\vec{\sigma}\|)) \end{aligned} \tag{3.18}$$

Note these dynamics are now in the form $\xi' = F(\xi;\epsilon) = f(\xi) + \epsilon\cdot v(\xi)$, that is (3.1) with $\xi = [\theta,\sigma_1,\dots,\sigma_n]^T$, $f(\xi) = [1,\kappa_2\sigma_2,\dots,\kappa_n\sigma_n]^T$, and

$$v(\xi) = [\mathbf{Z}(\xi),\mathbf{I}^{(2)}(\xi),\dots,\mathbf{I}^{(n)}(\xi)]^T u(\gamma(t;0) + \mathcal{O}(\|\vec{\sigma}\|)).$$

Therefore, the iSRC equation, for this particular system, reads

$$\gamma_1'(t) = \begin{bmatrix} 0 & & & \\ & \kappa_2 & & \\ & & \ddots & \\ & & & \kappa_n \end{bmatrix} \gamma_1(t) + \nu_1 \begin{bmatrix} 1 \\ 0 \\ \vdots \\ 0 \end{bmatrix} + \begin{bmatrix} Z_0(t)\cdot u(\gamma(t;0)) \\ I_0^{(2)}(t)\cdot u(\gamma(t;0)) \\ \vdots \\ I_0^{(n)}(t)\cdot u(\gamma(t;0)) \end{bmatrix} \tag{3.19}$$

The $\mathcal{O}(\|\vec{\sigma}\|)$ terms of the iPRC, iIRC, and the argument of u do not appear in (3.19) because we evaluate on the unperturbed limit-cycle solution, where the amplitude coordinates are zero. The resulting n equations are linear and uncoupled. Integration over one period with initial condition $\gamma_1(0) = p_1$ (specified by an arbitrary choice of Poincaré section) gives the result. □

We remark that computation of the iSRC in phase-amplitude coordinates is more efficient than in Cartesian coordinates because solving a system of ODEs is not necessary. One need only integrate the inner product of the iPRC or iIRC with the given perturbation $u(\mathbf{x})$. Appendix E compares our Theorem 3.1 to related results in [71].

The form of the solution provides a direct relation between the iSRC and the iPRC and iIRC. Theorem 3.1 establishes that the components of the infinitesimal shape-response curve, when expressed in phase-amplitude coordinates, are directly related to the inner products of the infinitesimal isostable response curves with the static perturbation $u(\mathbf{x})$. The phase component of the iSRC is a sum of three terms: the constant offset $(p_1)_1$ arises from the arbitrary choice of initial phase, the term $\nu_1 t$ denotes a constant rate of increase, accounting for a linear change in frequency given by ν_1, and the integral term highlights the role of the iPRC in describing the phase shift of the perturbed system with respect to the unperturbed system. The amplitude components of the iSRC are a sum of two terms: the term $\exp(\kappa_j t)(p_1)_j$ describes an exponential decay to the limit cycle, which is balanced by a transverse expansion due to the perturbation given by the integral term with the iIRC.

Note that there exist systems with a well defined iSRC that do not admit a phase-amplitude reduction to arbitrarily high order. For example, the system

$$\begin{aligned} x' &= x - x^3 - y + \epsilon \\ y' &= x + a|x|^{3/2} \end{aligned} \tag{3.20}$$

with $a = -0.7$ satisfies the single oscillator iSRC assumptions (B1-B3) and therefore admits a well-defined iSRC. However, the system (3.20) *does not* admit a phase-amplitude reduction via the parameterization method (or by Taylor expansions) to arbitrary order because assumption (C1) is not met. Specifically, the term $|x|^{3/2}$ does not admit well defined derivatives (of order 2 or greater) on the limit-cycle solution (the derivatives are not defined at $x = 0$). Because the high order phase-amplitude reduction methods require f to be differentiable arbitrarily many times on the limit-cycle solution to achieve a reduction of arbitrarily high order, both methods will fail. We remark that one could implement a phase-amplitude reduction for system (3.20) up to 1st order. However, such a reduction is of limited use because higher order terms are necessary, in general, to obtain an accurate representation of the dynamics.

The phase-amplitude reduction assumptions (A1-A3) pertain only to the unperturbed system ($\epsilon = 0$). To state that a system which admits a phase-amplitude reduction also admits a well-defined iSRC, one must consider the perturbation $u(\mathbf{x})$ on a case by case basis and verify the single oscillator iSRC assumptions (B1-B3).

3.1. iSRC Initial Condition. Here, we derive an expression for the initial condition, p_1, as the solution to a linear system. Subsequently, we show that in phase-amplitude coordinates, the linear system for p_1 admits a simple form.

LEMMA 3.4. *Under the single oscillator iSRC assumptions (B1-B3), and with a choice of Poincaré section transverse to the flow of the unperturbed system at the base point, the system (3.1) admits an iSRC with initial condition p_1, given as the solution* *to the linear system*

$$(I-M)p_1 = M\int_0^T \Phi(0,s)\left[\nu_1 f(\gamma(s;0)) + \left.\frac{\partial F(\gamma(s;0);\epsilon)}{\partial \epsilon}\right|_{\epsilon=0}\right]ds$$
$$\vec{n}\cdot p_1 = 0 \tag{3.21}$$

where M is the monodromy matrix, $\Phi(t,t_0)$ is the fundamental matrix solution, and $\vec{n}$ is the normal vector of the chosen Poincaré section. Furthermore, the system (3.21) is non-singular and hence specifies a unique initial condition.

Proof. For convenience, express the iSRC equation in simplified notation

$$\gamma_1' = A(t)\gamma_1 + b(t), \quad A(t)\equiv Df(\gamma(t;0)), \quad b(t)\equiv \nu_1 f(\gamma(t;0)) + \left.\frac{\partial F(\gamma(t;0);\epsilon)}{\partial\epsilon}\right|_{\epsilon=0} \tag{3.22}$$

The solution to such a periodic linear inhomogeneous equation is expressed as [4]

$$\gamma_1(t) = \Phi(t,0)\left[\gamma_1(0) + \int_0^t \Phi(0,s)b(s)ds\right] \tag{3.23}$$

Note that $\Phi(0,s)$ is the inverse of the fundamental matrix solution.

Suppose that the true initial condition is given by $\gamma_1(0) = p_1$. It must be that $\gamma_1(T) = p_1$ by the periodicity of $\gamma_1(t)$. Substitution and simplification gives

$$(I-M)p_1 = M\int_0^T \Phi(0,s)b(s)ds \tag{3.24}$$

This is a linear system, but it is singular as the monodromy matrix has a unitary eigenvalue. We remove this degree of freedom by considering the modified system

$$(I-M)p_1 = M\int_0^T \Phi(0,s)b(s)ds$$
$$\vec{n}\cdot p_1 = 0 \tag{3.25}$$

where $\vec{n}$ is the normal vector to the Poincare section chosen for the problem. We now show that this modified linear system is non-singular.

It is clear that $\dim \operatorname{null}(I-M) = 1$ by the linear asymptotic stability of the limit cycle. However, we can further characterize the nullspace of $I-M$ by recognizing that any vector $v\in \operatorname{null}(I-M)$ is an eigenvector associated with the unit eigenvalue of M. This vector is none other than the velocity at the base point on the unperturbed limit cycle, $f(\mathbf{x}_0)$. Consequently, all such vectors v satisfy

$$v = kf(\mathbf{x}_0), \quad k\in\mathbb{R} \tag{3.26}$$

By assumption, the chosen Poincaré section is transverse to the flow at $\mathbf{x}_0$. It follows that the section cannot be tangent to the flow at $\mathbf{x}_0$, which implies that

$$\vec{n}\cdot v \neq 0, \quad v\in \operatorname{null}(I-M) \tag{3.27}$$

Denote

$$\mathscr{M} = \begin{bmatrix} I-M \\ \vec{n}^T \end{bmatrix} \tag{3.28}$$

Suppose by contradiction that $\mathscr{M}$ is singular. Then, there must exist some $y \neq 0$ such that $\mathscr{M}y = 0$. That is, we have simultaneously

$$(I - M)y = 0, \quad \vec{n}^T y = 0 \tag{3.29}$$

From the first equation, $y \in \text{null}(I - M)$, which implies that $\vec{n}^T y \neq 0$, contradicting the second equation. Hence, the equation (3.21) is a linear system with a trivial nullspace and thus specifies a unique solution. ∎

We now show that this system simplifies in phase-amplitude coordinates.

Lemma 3.5. *Under the iSRC phase-amplitude assumptions (C1-C3), the iSRC initial condition, p_1, in phase-amplitude coordinates, satisfies a linear system*

$$\begin{bmatrix} 0 & & & \\ & 1 - e^{(\kappa_2 T)} & & \\ & & \ddots & \\ & & & 1 - e^{(\kappa_n T)} \\ & & \vec{n} & \end{bmatrix} p_1 = \begin{bmatrix} 0 \\ \int_0^T e^{(\kappa_2 (T-s))} \left(I_0^{(2)}(s) \cdot u(\gamma(s;0)) \right) ds \\ \vdots \\ \int_0^T e^{(\kappa_n (T-s))} \left(I_0^{(n)}(s) \cdot u(\gamma(s;0)) \right) ds \\ 0 \end{bmatrix} \tag{3.30}$$

where $\vec{n}$ is a vector normal to the Poincaré section transverse to the flow of the unperturbed system at the intersection point.

Proof. Observe that in phase-amplitude coordinates

$$\Phi(t,0) = \begin{bmatrix} 1 & & & \\ & e^{(\kappa_2 t)} & & \\ & & \ddots & \\ & & & e^{(\kappa_n t)} \end{bmatrix}, \quad \left. \frac{\partial F(\gamma(t;0);\epsilon)}{\partial \epsilon} \right|_{\epsilon=0} = \begin{bmatrix} Z_0(t) \cdot u(\gamma(t;0);0) \\ I_0^{(2)}(t) \cdot u(\gamma(t;0);0) \\ \vdots \\ I_0^{(n)}(t) \cdot u(\gamma(t;0);0) \end{bmatrix} \tag{3.31}$$

The result follows from rewriting equation (3.21) in phase-amplitude coordinates. ∎

The form of the linear system in phase-amplitude coordinates underlines why the system is singular. While the amplitude coordinates of the initial condition are uniquely specified, the initial phase is arbitrary. To fix a unique initial condition, one must in turn fix an appropriate Poincaré section. Mathematically, this is accomplished by choosing an appropriate normal vector $\vec{n}$.

Often, a specific choice of Poincaré section is well-suited for a particular problem. In neuron oscillator models, it is a common convention to fix a reference phase when the voltage component reaches a maximum [16]. Other systems admit limit-cycle solutions which may be divided into regions [67]. The dividers in each of these systems are natural candidates for a particular choice of Poincaré section. In phase-amplitude coordinates, it is straightforward to choose an isochron of the system as a Poincaré section. One need only choose the vector normal to the flow of the phase. In two dimensions, one would choose a section spanned by $\vec{q} = (0, 1)$ (see Figure 3.1).

Choosing the Poincaré section to be an isochron of the original system corresponds to setting $n_1 = [1, 0, \ldots, 0]$, hence the first component of p_1 (the phase shift) must be identically zero. The remaining components are determined by the 2nd through $(n+1)$st rows of (3.30).

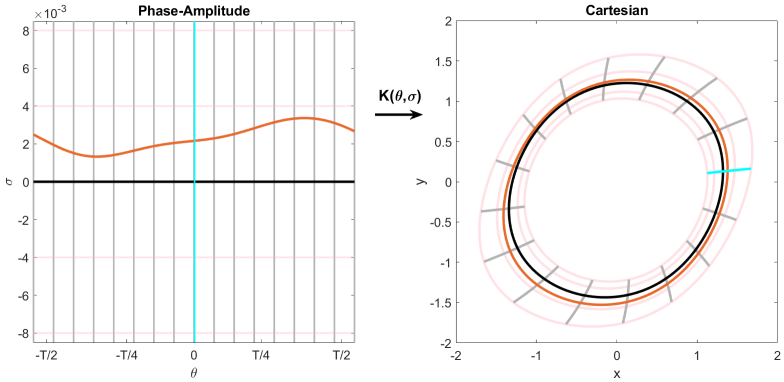

FIGURE 3.1. *Limit-cycle dynamics in phase-amplitude coordinates (left) and Cartesian coordinates (right). Shown are an unperturbed limit cycle (black) and a perturbed limit cycle (orange) overlayed with isochrons (gray) and isostable level curves (pink). An isochron is chosen as a particular choice of Poincaré section (cyan). The dynamics are considerably simplified in phase-amplitude coordinates as opposed to Cartesian coordinates. The dynamics correspond to the simplified circadian rhythm model considered in §4.4.*

The computation of the initial condition is efficient in phase-amplitude coordinates. In Cartesian coordinates, one must solve an ODE (the variational equation) to obtain the fundamental matrix solution at each time-step. One must also invert the fundamental matrix solution at each time-step, which can introduce numerical errors if ill-conditioned. In phase-amplitude coordinates, one need only compute integrals.

Theorem 3.1 and Lemma 3.5 show that iSRC computations simplify dramatically in phase-amplitude coordinates, regardless of the system's dimension. Methods exist for mapping the result to the original Cartesian coordinates, i.e., Eq. (2.9), yet often involve non-trivial computations for high-dimensional systems [46, 49, 72].

3.2. iSRC Equation (Coupled Oscillators with Identical Periods). In this section, we consider applications of the iSRC and phase-amplitude reduction to systems of two coupled oscillators with identical periods. Formally, we consider an n-dimensional system

$$\begin{bmatrix}\mathbf{x}'\\ \mathbf{y}'\end{bmatrix} = \begin{bmatrix}F(\mathbf{x},\mathbf{y};\delta)\\ G(\mathbf{y},\mathbf{x};\delta)\end{bmatrix} = \begin{bmatrix}f(\mathbf{x})\\ g(\mathbf{y})\end{bmatrix} + \delta\begin{bmatrix}u_f(\mathbf{x},\mathbf{y})\\ u_g(\mathbf{y},\mathbf{x})\end{bmatrix} \tag{3.32}$$

with $\mathbf{x} \in \mathbb{R}^p$, $\mathbf{y} \in \mathbb{R}^q$, $p + q = n$, and where $u_f(\mathbf{x}, \mathbf{y})$ and $u_g(\mathbf{y}, \mathbf{x})$ are coupling functions with strength δ. By letting $\mathbf{z} = [\mathbf{x}^T\ \mathbf{y}^T]^T$ and $u(\mathbf{z}) = [u_f(\mathbf{x}, \mathbf{y})^T\ u_g(\mathbf{y}, \mathbf{x})^T]^T$ we express (3.32) more concisely as

$$\mathbf{z}' = H(\mathbf{z}, \delta) = h(\mathbf{z}) + \delta \cdot u(\mathbf{z}) \tag{3.33}$$

We consider only cases where the uncoupled dynamics ($\delta = 0$) admit non-constant limit-cycle solutions, $\gamma_f(t; 0)$ and $\gamma_g(t; 0)$. It is possible to introduce an arbitrary phase shift into one of the uncoupled limit cycles, and therefore none of the n-dimensional orbits are limit cycles when $\delta = 0$ because they are neither unique nor isolated.

We are interested in studying (3.32-3.33) in the case of 1:1 mode-locked solutions (for $\delta \neq 0$), by which we mean a non-constant stable limit cycle $\mathbf{z}(t) = \gamma(t; \delta)$ characterized by the property that the corresponding coupled trajectories of the f and g dynamics have the same (minimal) period.

Lemma 3.6. *Consider a system of the form (3.33) and assume that the coupled oscillator iSRC assumptions hold:*

- *(D1) There exists an open subset $\Omega \subset \mathbb{R}^n$ and an open neighborhood of zero $\mathcal{I} \subset \mathbb{R}$ such that the vector field $H(\mathbf{z};\delta) : \Omega \times \mathcal{I} \to \mathbb{R}^n$ is $\mathcal{C}^1$ in both the coordinates $\mathbf{z} \subset \Omega$ and the perturbation strength $\delta \in \mathcal{I}$.*
- *(D2) When $\delta = 0$, the uncoupled dynamics admit non-constant linearly asymptotically stable limit-cycle solutions, $\gamma_f(t;0)$ and $\gamma_g(t;0)$, of period T.*
- *(D3) For $\delta \in \mathcal{I} \setminus \{0\}$, system (3.33) admits a unique linearly asymptotically stable limit cycle, $\gamma(t;\delta) \in \Omega$, corresponding to a 1:1 mode locked solution.*
- *(D4) The period of the 1:1 mode-locked solution is given by $T(\delta)$, which has C^1 dependence in $\delta \in \mathcal{I}$, and satisfies $\lim_{\delta \to 0} T(\delta) = T$.*

Then, (3.33) has a well-defined iSRC which is expressed as set of uncoupled equations

$$
(\gamma_1^{(f)})' = Df(\gamma_f(t;0))\gamma_1^{(f)} + \nu_1 f(\gamma_f(t;0)) + \left.\frac{\partial F(\gamma_f(t;0), \gamma_g(t+\Delta;0);\delta)}{\partial \delta}\right|_{\delta=0}
$$
$$
(\gamma_1^{(g)})' = Dg(\gamma_g(t+\Delta;0))\gamma_1^{(g)} + \nu_1 g(\gamma_g(t+\Delta;0)) + \left.\frac{\partial G(\gamma_g(t+\Delta;0), \gamma_f(t;0);\delta)}{\partial \delta}\right|_{\delta=0} \tag{3.34}
$$

The linear shift in frequency, ν_1, and the constant phase-shift, Δ, are uniquely determined by the equations

$$
\begin{aligned}
\nu_1 &= -\frac{1}{T}\int_0^T (Z_0^{(f)}(s))^T \left.\frac{\partial F(\gamma_f(s;0), \gamma_g(s+\Delta;0);\delta)}{\partial \delta}\right|_{\delta=0} ds \\
&= -\frac{1}{T}\int_0^T (Z_0^{(g)}(s+\Delta))^T \left.\frac{\partial G(\gamma_g(s+\Delta;0), \gamma_f(s;0);\delta)}{\partial \delta}\right|_{\delta=0} ds
\end{aligned} \tag{3.35}
$$

The initial condition for (3.34) is discussed in more detail after the proof.

Proof. Note that *a priori*, the uncoupled oscillators have an arbitrary phase offset. Explicitly, denote the time variable for the first oscillator as $t_1 = t + \phi_1$ and for the second oscillator as $t_2 = t + \phi_2$, where $\phi_1, \phi_2 \in [0, T)$ are constant phase offsets determined by a particular choice of base points, $\mathbf{x}_0$ and $\mathbf{y}_0$, respectively. Define new time variables, $\tau_i(t) = \omega t_i$ for some $\omega \in \mathbb{R}$ to be determined. In these new coordinates, written as $\mathbf{x}(\tau_{\mathbf{1}}(\mathbf{t});\delta)$ and $\mathbf{y}(\tau_2(t);\delta)$, the solution of (3.32) obeys

$$
\begin{aligned}
\omega \frac{d\mathbf{x}}{d\tau_1} &= F(\mathbf{x}, \mathbf{y}; \delta) \\
\omega \frac{d\mathbf{y}}{d\tau_2} &= G(\mathbf{y}, \mathbf{x}; \delta)
\end{aligned} \tag{3.36}
$$

Assumptions (D1-D4) guarantee a solution of the form

$$
\begin{aligned}
\mathbf{x}(\tau_1(t);\delta) &= \gamma_f(t+\phi_1;0) + \delta\gamma_1^{(f)}(t) + \mathcal{O}(\delta^2) \quad \text{(uniformly in } t) \\
\mathbf{y}(\tau_2(t);\delta) &= \gamma_g(t+\phi_2;0) + \delta\gamma_1^{(g)}(t) + \mathcal{O}(\delta^2) \quad \text{(uniformly in } t) \\
\omega &= 1 + \delta\omega_1 + \mathcal{O}(\delta^2)
\end{aligned} \tag{3.37}
$$

for certain values of $\phi_2 - \phi_1$, to be determined in the following. Substituting (3.37) into (3.36) for the $\mathbf{x}$ dynamics gives, for the LHS

$$\begin{aligned} \omega \frac{d\mathbf{x}}{d\tau_1} &= \left(1 + \delta\omega_1 + \mathcal{O}(\delta^2)\right) \frac{d}{dt}\left[\gamma_f(t+\phi_1;0) + \delta\gamma_1^{(f)}(t) + \mathcal{O}(\delta^2)\right] \\ &= f(\gamma_f(t+\phi_1;0)) + \delta\left[\omega_1 f(\gamma_f(t+\phi_1;0)) + (\gamma_1^{(f)}(t))'\right] + \mathcal{O}(\delta^2) \end{aligned} \tag{3.38}$$

and for the RHS

$$\begin{aligned} F(\mathbf{x},\mathbf{y};\delta) &= F(\gamma_f(t+\phi_1;0) + \delta\gamma_1^{(f)}(t) + \mathcal{O}(\delta^2), \gamma_g(t+\phi_2;0) + \delta\gamma_1^{(g)}(t) + \mathcal{O}(\delta^2);\delta) \\ &= F(\gamma_f(t+\phi_1;0), \gamma_g(t+\phi_2;0);0) \\ &\qquad + \delta \frac{dF}{d\delta}(\gamma_f(t+\phi_1;0), \gamma_g(t+\phi_2;0);\delta)\bigg|_{\delta=0} + \mathcal{O}(\delta^2) \\ &= F(\gamma_f(t+\phi_1;0), \gamma_g(t+\phi_2;0);0) \\ &\qquad + \delta\left[\frac{\partial F}{\partial \mathbf{x}}\frac{d\mathbf{x}}{d\delta} + \frac{\partial F}{\partial \mathbf{y}}\frac{d\mathbf{y}}{d\delta} + \frac{\partial F}{\partial \delta}\right](\gamma_f(t+\phi_1;0), \gamma_g(t+\phi_2;0);\delta)\Big|_{\delta=0} + \mathcal{O}(\delta^2) \end{aligned} \tag{3.39}$$

Note that $F(\gamma_f(t+\phi_1;0), \gamma_g(t+\phi_2;0);0) = F(\gamma_f(t+\phi_1;0),0;0) = f(\gamma_f(t+\phi_1;0))$ because the $\mathbf{y}$ dependence arises only for $\delta \neq 0$. Equating the two sides (neglecting higher order terms) and simplifying gives

$$\begin{aligned} \omega_1 f(\gamma_f(t+\phi_1;0)) + (\gamma_1^{(f)})' = Df(\gamma_f(t+\phi_1;0))\gamma_1^{(f)} &+ 0 \\ &+ \frac{\partial F(\gamma_f(t+\phi_1;0), \gamma_g(t+\phi_2;0);\delta)}{\partial \delta}\bigg|_{\delta=0} \end{aligned} \tag{3.40}$$

The analysis for the $\mathbf{y}$ dynamics is similar. We find that

$$\begin{aligned} (\gamma_1^{(f)})' - Df(\gamma_f(t+\phi_1;0))\gamma_1^{(f)} &= -\omega_1 f(\gamma_f(t+\phi_1;0)) \\ &\qquad + \frac{\partial F(\gamma_f(t+\phi_1;0), \gamma_g(t+\phi_2;0);\delta)}{\partial \delta}\bigg|_{\delta=0} \\ (\gamma_1^{(g)})' - Dg(\gamma_g(t+\phi_2;0))\gamma_1^{(g)} &= -\omega_1 g(\gamma_g(t+\phi_2;0)) \\ &\qquad + \frac{\partial G(\gamma_g(t+\phi_2;0), \gamma_f(t+\phi_1;0);\delta)}{\partial \delta}\bigg|_{\delta=0} \end{aligned} \tag{3.41}$$

The full system can be expressed as a block n-dimensional system

$$\begin{aligned} \begin{bmatrix} \gamma_1^{(f)} \\ \gamma_1^{(g)} \end{bmatrix}' = \begin{bmatrix} Df(\gamma_f(t+\phi_1;0)) & 0 \\ 0 & Dg(\gamma_g(t+\phi_2;0)) \end{bmatrix} \begin{bmatrix} \gamma_1^{(f)} \\ \gamma_1^{(g)} \end{bmatrix} &- \omega_1 \begin{bmatrix} f(\gamma_f(t+\phi_1;0)) \\ g(\gamma_g(t+\phi_2;0)) \end{bmatrix} \\ &+ \begin{bmatrix} \frac{\partial F(\gamma_f(t+\phi_1;0), \gamma_g(t+\phi_2;0);\delta)}{\partial \delta} \\ \frac{\partial G(\gamma_g(t+\phi_2;0), \gamma_f(t+\phi_1;0);\delta)}{\partial \delta} \end{bmatrix}\Bigg|_{\delta=0} \end{aligned} \tag{3.42}$$

We find a solvability condition for (3.42) by employing the Fredholm alternative. The operator acting on the iSRC is given by

$$L\begin{bmatrix}\gamma_1^{(f)}\\ \gamma_1^{(g)}\end{bmatrix} = \left(\frac{d}{dt} - \begin{bmatrix}Df(\gamma_f(t+\phi_1;0)) & 0\\ 0 & Dg(\gamma_g(t+\phi_2;0))\end{bmatrix}\right)\begin{bmatrix}\gamma_1^{(f)}\\ \gamma_1^{(g)}\end{bmatrix} \tag{3.43}$$

along with T-periodic boundary conditions. The adjoint is given by

$$L^\dagger\begin{bmatrix}\gamma_1^{(f)}\\ \gamma_1^{(g)}\end{bmatrix} = \left(-\frac{d}{dt} - \begin{bmatrix}Df(\gamma_f(t+\phi_1;0)) & 0\\ 0 & Dg(\gamma_g(t+\phi_2;0))\end{bmatrix}^T\right)\begin{bmatrix}\gamma_1^{(f)}\\ \gamma_1^{(g)}\end{bmatrix} \tag{3.44}$$

Notice that the nullspace of the adjoint operator is two-dimensional, with

$$\operatorname{span}\Big(\operatorname{null}(L^\dagger)\Big) = \operatorname{span}\left\{\begin{bmatrix}Z_0^{(f)}(t+\phi_1)\\ 0\end{bmatrix}, \begin{bmatrix}0\\ Z_0^{(g)}(t+\phi_2)\end{bmatrix}\right\} \tag{3.45}$$

where $Z_0^{(f)}$ and $Z_0^{(g)}$ are the iPRCs of the first and second oscillators, respectively. The Fredholm alternative establishes a solvability condition for a T-periodic solution by enforcing the simultaneous orthogonality of the inhomogenous term in (3.42) with both spanning vectors of the nullspace of $L^\dagger$

$$\begin{aligned}
0 &= \int_0^T \begin{bmatrix}Z_0^{(f)}(t+\phi_1)\\ 0\end{bmatrix}^T \Bigg(-\omega_1 \begin{bmatrix}f(\gamma_f(t+\phi_1;0))\\ g(\gamma_g(t+\phi_2;0))\end{bmatrix} \\
&\qquad + \begin{bmatrix}\frac{\partial F(\gamma_f(t+\phi_1;0),\gamma_g(t+\phi_2;0);\delta)}{\partial\delta}\\ \frac{\partial G(\gamma_g(t+\phi_2;0),\gamma_f(t+\phi_1;0);\delta)}{\partial\delta}\end{bmatrix}\Bigg|_{\delta=0}\Bigg) dt \\
0 &= \int_0^T \begin{bmatrix}0\\ Z_0^{(g)}(t+\phi_2)\end{bmatrix}^T \Bigg(-\omega_1 \begin{bmatrix}f(\gamma_f(t+\phi_1;0))\\ g(\gamma_g(t+\phi_2;0))\end{bmatrix} \\
&\qquad + \begin{bmatrix}\frac{\partial F(\gamma_f(t+\phi_1;0),\gamma_g(t+\phi_2;0);\delta)}{\partial\delta}\\ \frac{\partial G(\gamma_g(t+\phi_2;0),\gamma_f(t+\phi_1;0);\delta)}{\partial\delta}\end{bmatrix}\Bigg|_{\delta=0}\Bigg) dt
\end{aligned} \tag{3.46}$$

Simplification of the orthogonality condition reveals that

$$\begin{aligned}
0 &= \int_0^T (Z_0^{(f)}(t+\phi_1))^T \Bigg(-\omega_1 f(\gamma_f(t+\phi_1;0)) \\
&\qquad + \frac{\partial F(\gamma_f(t+\phi_1;0),\gamma_g(t+\phi_2;0);\delta)}{\partial\delta}\Bigg|_{\delta=0}\Bigg) dt \\
0 &= \int_0^T (Z_0^{(g)}(t+\phi_2))^T \Bigg(-\omega_1 g(\gamma_g(t+\phi_2;0)) \\
&\qquad + \frac{\partial G(\gamma_g(t+\phi_2;0),\gamma_f(t+\phi_1;0);\delta)}{\partial\delta}\Bigg|_{\delta=0}\Bigg) dt
\end{aligned} \tag{3.47}$$

Rearranging gives

$$
\omega_1 = \frac{\int_0^T (Z_0^{(f)}(t+\phi_1))^T \frac{\partial F(\gamma_f(t+\phi_1;0),\gamma_g(t+\phi_2;0);\delta)}{\partial\delta}\Big|_{\delta=0} dt}{\int_0^{T_f} (Z_0^{(f)}(t+\phi_1))^T f(\gamma(t+\phi_1;0))dt}
\tag{3.48}
$$
$$
\omega_1 = \frac{\int_0^T (Z_0^{(g)}(t+\phi_2))^T \frac{\partial G(\gamma_g(t+\phi_2;0),\gamma_f(t+\phi_1;0);\delta)}{\partial\delta}\Big|_{\delta=0} dt}{\int_0^{T_g} (Z_0^{(g)}(t+\phi_2))^T g(\gamma(t+\phi_2;0))dt}
$$

Equating the expressions for ω_1, and exploiting periodicity, gives

$$
\begin{aligned}
\int_0^T (Z_0^{(f)}(s))^T \frac{\partial F(\gamma_f(s;0),\gamma_g(s+\phi_2-\phi_1;0);\delta)}{\partial\delta}\Big|_{\delta=0} ds \\
= \int_0^T (Z_0^{(g)}(s))^T \frac{\partial G(\gamma_g(s;0),\gamma_f(s+\phi_1-\phi_2;0);\delta)}{\partial\delta}\Big|_{\delta=0} ds
\end{aligned}
\tag{3.49}
$$

For convenience, we introduce the notation

$$
\begin{aligned}
H_f(\alpha) &= \int_0^T (Z_0^{(f)}(s))^T \frac{\partial F(\gamma_f(s;0),\gamma_g(s+\alpha;0);\delta)}{\partial\delta}\Big|_{\delta=0} ds \\
H_g(\alpha) &= \int_0^T (Z_0^{(g)}(s))^T \frac{\partial G(\gamma_g(s;0),\gamma_f(s+\alpha;0);\delta)}{\partial\delta}\Big|_{\delta=0} ds
\end{aligned}
\tag{3.50}
$$

In this notation, equation (3.49) becomes

$$
H_g(-\psi) - H_f(\psi) = 0 \tag{3.51}
$$

where $\psi = \phi_2 - \phi_1$ denotes the difference of the phases. Note that the roots of this equation are equivalent to the fixed points of the ODE

$$
\psi' = \delta[H_g(-\psi) - H_f(\psi)] \tag{3.52}
$$

a familiar result from weakly coupled oscillator theory [16]. As in the classical theory, (un)stable fixed points of (3.52) correspond to (un)stable periodic orbits of the full equations (3.32), to linear order in δ. By assumption (D3) (unique linearly asymptotically stable 1:1 mode-locked solution) the equation (3.52) is guaranteed to have a unique stable fixed point, $\psi^* = \Delta$, corresponding to a fixed phase offset. Given this value of Δ, one can determine ω_1 by either of the equations in (3.49).

Without loss of generality, and for ease of notation, we may choose the phase constants ϕ_1 and ϕ_2 so that $\phi_1 = 0$ and $\phi_2 = \Delta$. Then, the linear change in frequency of the system is given by

$$
\begin{aligned}
\nu_1 &= -\frac{1}{T}\int_0^T (Z_0^{(f)}(s))^T \frac{\partial F(\gamma_f(s;0),\gamma_g(s+\Delta;0);\delta)}{\partial\delta}\Big|_{\delta=0} ds \\
&= -\frac{1}{T}\int_0^T (Z_0^{(g)}(s+\Delta))^T \frac{\partial G(\gamma_g(s+\Delta;0),\gamma_f(s;0);\delta)}{\partial\delta}\Big|_{\delta=0} ds
\end{aligned}
\tag{3.53}
$$

and, as was to be shown, the iSRC for the n-dimensional system is given by

$$\begin{bmatrix}\gamma_1^{(f)}\\ \gamma_1^{(g)}\end{bmatrix}' = \begin{bmatrix}Df(\gamma_f(t;0)) & 0\\ 0 & Dg(\gamma_g(t+\Delta;0))\end{bmatrix}\begin{bmatrix}\gamma_1^{(f)}\\ \gamma_1^{(g)}\end{bmatrix} + \nu_1\begin{bmatrix}f(\gamma_f(t;0))\\ g(\gamma_g(t+\Delta;0))\end{bmatrix} + \begin{bmatrix}\frac{\partial F(\gamma_f(t;0),\gamma_g(t+\Delta;0);\delta)}{\partial\delta}\\ \frac{\partial G(\gamma_g(t+\Delta;0),\gamma_f(t;0);\delta)}{\partial\delta}\end{bmatrix}\Bigg|_{\delta=0} \tag{3.54}$$

□

Although our proof leverages elements of the classical theory of weakly coupled oscillators [16], to the best of our knowledge the iSRC for weakly coupled oscillators has not been previously described. We showed that the iSRC for the coupled system can be expressed as a system of uncoupled iSRCs corresponding to each of the oscillators. To compute the initial condition, one must specify an appropriate Poincaré section for the full n-dimensional system, in the sense of (2.18). We repeat that this section must be transverse to the flow of the uncoupled system at the initial condition and must intersect the perturbed orbit. In contrast to single oscillators, the coupled system consists of perturbed trajectories corresponding to both oscillators which, in general, have a certain phase-lag. Any intersection point on the perturbed orbit, specified by a particular choice of section, must be chosen consistently to respect the phase-lag of the true perturbed orbit. Given an appropriate choice of section, the initial conditions for the uncoupled iSRC equations can be computed as for a single oscillator by using the corresponding components of the normal vector for each computation.

The frequency matching condition (3.49) can be used as a test to determine if a system admits a 1:1 mode-locked solution for arbitrarily small coupling strengths. By the assumed existence of such a solution, there must exist a phase offset Δ so that the equations are consistent. A lack of consistency indicates that such a solution does not exist. Appendix B in the supplementary materials contains several examples of analytically tractable systems to demonstrate this point.

Implementing a phase-amplitude reduction for an n-dimensional system with $n \geq 4$ is numerically challenging. It is significant that the iSRC for a system of two coupled oscillators with identical periods can be deflated into a system of uncoupled equations corresponding to each oscillator. In practice, one need only implement a phase-amplitude reduction for each of the individual oscillators (provided that the phase-amplitude reduction assumptions (A1-A3) hold for each oscillator), allowing for the study of systems of higher dimensionality using the phase-amplitude framework.

3.3. iSRC Equation (Coupled Oscillators with Non-Identical Periods). In this section, we apply the iSRC analysis to systems of two coupled oscillators with non-identical periods. We begin by noting that the condition of non-identical periods complicates an asymptotic analysis in the style presented above. For systems of two coupled oscillators with identical periods, a 1:1 mode locked solution is expected for arbitrarily small coupling strengths, δ. In the case of oscillators with different natural periods, a 1:1 mode-locked solution is expected to break down as the coupling strength δ tends to zero [23] (see Figure 3.2). In such a case, assumption (D4) does not hold because the period $T(\delta)$ does not depend continuously on δ. Here, we provide an asymptotic approach that circumvents the continuity issue, and demonstrate that the iSRC for the system with non-identical periods is a linear combination of two iSRCs: one corresponding to the shape change induced by the coupling, and another corresponding to the shape change induced by the timing difference of the oscillators.

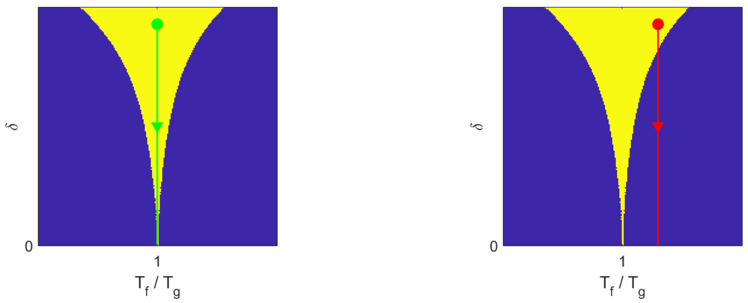

FIGURE 3.2. *The Arnold tongue for a 4D system: a 2D Stuart-Landau oscillator coupled to a 2D Van der Pol oscillator (see §4.3). The yellow region corresponds to parameter values for which the system admits a stable 1:1 mode-locked solution.* ***Left:*** *In the case of oscillators with identical periods (Lemma 3.6), a 1:1 mode-locked solution is expected for any value of the coupling strength, δ.* ***Right:*** *In the case of oscillators with different natural periods (Theorem 3.7), the 1:1 mode-locked solution is expected to break down as $\delta \to 0$.*

THEOREM 3.7. *Consider a system of two coupled oscillators*

$$\begin{aligned} \mathbf{x}' &= F(\mathbf{x}, \mathbf{y}; \delta) = f(\mathbf{x}) + \delta \cdot u_f(\mathbf{x}, \mathbf{y}) \\ \mathbf{y}' &= G(\mathbf{y}, \mathbf{x}; \delta) = g(\mathbf{y}) + \delta \cdot u_g(\mathbf{y}, \mathbf{x}) \end{aligned} \tag{3.55}$$

with $\mathbf{x} \in \mathbb{R}^p$, $\mathbf{y} \in \mathbb{R}^q$, and $p+q = n$. Assume that when $\delta = 0$, the uncoupled dynamics admit linearly asymptotically stable limit-cycle solutions, $\mathbf{x}(t) = \gamma_f(t) = \gamma_f(t + T_f)$ and $\mathbf{y}(t) = \gamma_g(t) = \gamma_g(t + T_g)$, with $T_g \geq T_f$. Assume further that there exists an open subset $\mathcal{J} \subset \mathbb{R} \setminus \{0\}$ such that for every $\delta \in \mathcal{J}$, (3.55) admits a unique linearly asymptotically stable 1:1 mode-locked solution. There are two cases:

- *(Identical periods) Assume that $T_f = T_g$, and further that (3.55) satisfies the coupled oscillator iSRC assumptions (D1-D4). Then, (3.55) admits a well-defined iSRC described by Lemma 3.6.*
- *(Non-identical periods) Assume that $T_f < T_g$, and that the related system*

$$\begin{aligned} x' &= \tilde{F}(\mathbf{x}, \mathbf{y}; \delta, \beta) = \left(\frac{T_f}{T_g} + \beta \right) f(\mathbf{x}) + \delta \cdot u_f(\mathbf{x}, \mathbf{y}) \\ y' &= G(\mathbf{y}, \mathbf{x}; \delta) = g(\mathbf{y}) + \delta \cdot u_g(\mathbf{y}, \mathbf{x}) \end{aligned} \tag{3.56}$$

  satisfies the following assumptions:
  - *For every $(\beta, \delta) \in [0,\ 1 - T_f/T_g] \times \mathcal{J}$,* (3.56) *admits a unique linearly asymptotically stable limit cycle, $\gamma(t; \delta, \beta)$, corresponding to a 1:1 mode-locked solution.*
  - *When $\beta = 0$ and $\delta = 0$,* (3.56) *satisfies the coupled oscillator iSRC assumptions (D1-D4).*
  - *When $\beta = 0$ and $\delta \in \mathcal{J}$,* (3.56) *satisfies the single oscillator iSRC assumptions (B1-B3).*

  Then, (3.55) admits a well-defined iSRC to linear order in both the parameters δ and β. The explicit form of the iSRC is specified in the proof to follow by equations (3.57), (3.59), *and* (3.63).

We make several clarifying remarks before proving Theorem 3.7. The related system (3.56) introduces a timing parameter, β, that shifts the frequency of one of the oscillators (one could choose to shift the frequency of either oscillator without loss of generality). As motivation, shifting the frequency of one of the oscillators maintains continuity of the period of the limit cycle (in the joint variables $\mathbf{z}$) as a function of the coupling strength, δ. This continuity ensures that our asymptotic analysis of the system does not break down (see Figure 3.3). Of interest are cases for which $\delta \in \mathcal{J}$ can be treated as a small parameter. In these cases, the existence of a unique asymptotically stable 1:1 mode-locked solution implies that the ratio of the periods of the two oscillators is small in the sense that $T_f/T_g \lesssim 1$ (see Figure 3.2). Therefore, the timing parameter, β, with $0 \leq \beta \leq 1 - T_f/T_g \ll 1$, can also be treated as a small parameter.

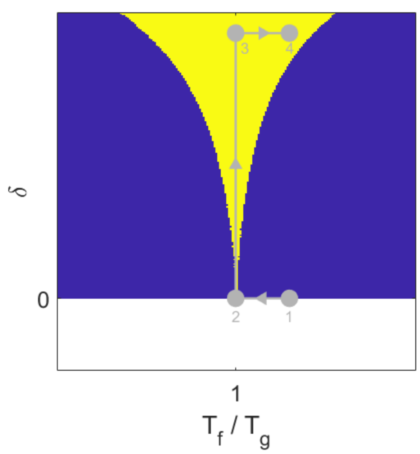

FIGURE 3.3. *The Arnold tongue corresponding to 1:1 mode locking for a 4D system: a 2D Stuart-Landau oscillator coupled to a 2D Van der Pol oscillator (see §4.3). The four steps outlined in the proof of Theorem 3.7 to compute the iSRC for coupled oscillators with non-identical periods are labeled.* ***Step 1:*** *The original system of uncoupled oscillators with non-identical periods.* ***Step 2:*** *Uncoupled oscillators with identical periods.* ***Step 3:*** *Coupled oscillators with identical periods (stable 1:1 mode-locked solution).* ***Step 4:*** *The true 1:1 mode-locked solution to be approximated by the four step iSRC analysis. Our analysis requires only horizontal and vertical shifts in parameter space; this guarantees that the period of the stable 1:1 mode-locked solution depends continuously on the coupling strength δ at all steps, and that our asymptotic analysis of the system remains valid.*

Conceptually, we begin at the point labelled “1” in Figure 3.3, where the two oscillators are uncoupled ($\delta = 0$) and have their original periods $T_f < T_g$. For ease of notation, define $\beta^* = 1 - T_f/T_g$. At point 1, $\beta = \beta^*$. From the assumptions of Theorem 3.7, the two oscillators will exhibit a single limit cycle with 1:1 mode locking upon increasing δ sufficiently to a fixed $\delta^* \in \mathcal{J}$, i.e., at point 4 in the (β, δ) plane (Figure 3.3). However, we cannot study how the coupling distorts the shape of the oscillators – via the iSRC – by directly introducing the coupling parameter, because any arc passing from the point 1 to point 4 passes through a region outside the 1:1 mode-locking Arnold tongue. In order to circumvent this difficulty, we pursue an alternative route. First, we shift the period of one of the oscillators (shifting β from β^* to zero) to move from point 1 to point 2. At point 2 we have two uncoupled oscillators with *identical periods*. But because we have only changed the first oscillator’s differential equation by multiplying with a decelerating prefactor, the shift from point 1 to point 2 has not changed the shape of the orbit. Next, we shift from point 2 to point 3 by introducing the coupling ($\delta \to \delta^*$). The iSRC relating the 1:1 mode-locked solution at point 3 to the uncoupled, identical-period oscillators at point 2 is given by Lemma 3.6. Finally, by *reaccelerating* the first oscillator back to its orignal period ($\beta \to \beta^*$) we recover the iSRC for the original system of interest: a 1:1 mode-locked system of two coupled oscillators with nonidentical periods.

The detailed proof of Theorem 3.7 follows.

Proof. In the case of identical periods, the proof is given by Lemma 3.6. If $T_f < T_g$, we analyze the iSRC of (3.55-3.56) in two steps (corresponding to the arrows $2 \to 3$ and $3 \to 4$ in Figure 3.3). Abusing notation, we denote the uncoupled limit-cycle dynamics $\gamma_f(t;0,\beta)$ and $\gamma_g(t;0,\beta)$, respectively.

Step 1: Fix $\beta = 0$ (point 2 in Fig. 3.3) and let $\delta \to \delta^* \in \mathcal{J}$ to couple the oscillators (point 2 $\to$ point 3). By assumption, the related system (3.56) with $\beta = 0$ and $\delta = \delta^*$ (coupled oscillators with identical periods) admits a unique linearly asymptotically stable 1:1 mode-locked solution, $\gamma(t;\delta^*,0) = \gamma(t+\mathcal{T};\delta^*,0)$. Furthermore, when $\beta = 0$ and $\delta = 0$ (uncoupled oscillators with identical periods), by Lemma 3.6, (3.56) admits a well-defined T_g-periodic iSRC corresponding to $\gamma(t;\delta^*,0)$, $\Upsilon_1(t) = [(\Upsilon_1^{(f)}(t))^T \ (\Upsilon_1^{(g)}(t))^T]^T$, which satisfies

$$
\begin{aligned}
(\Upsilon_1^{(f)})' &= D\tilde{f}(\gamma_f(t;0,0))\Upsilon_1^{(f)} + \nu_1 \tilde{f}(\gamma_f(t;0,0)) \\
&\qquad + \left.\frac{\partial \tilde{F}(\gamma_f(t;0,0),\gamma_g(t+\Delta;0);\delta,0)}{\partial \delta}\right|_{\delta=0} \\
(\Upsilon_1^{(g)})' &= Dg(\gamma_g(t+\Delta;0))\Upsilon_1^{(g)} + \nu_1 g(\gamma_g(t+\Delta;0)) \\
&\qquad + \left.\frac{\partial G(\gamma_g(t+\Delta;0),\gamma_f(t;0,0);\delta)}{\partial \delta}\right|_{\delta=0}
\end{aligned}
\tag{3.57}
$$

where $\tilde{f}(\mathbf{x}) = \frac{T_f}{T_g} f(\mathbf{x})$. The linear shift in frequency, ν_1, and the constant phase-shift, Δ, are determined by

$$
\begin{aligned}
\nu_1 &= -\frac{1}{T_g}\int_0^{T_g} (Z_0^{(\tilde{f})}(s))^T \left.\frac{\partial \tilde{F}(\gamma_f(s;0,0),\gamma_g(s+\Delta;0);\delta,0)}{\partial \delta}\right|_{\delta=0} ds \\
&= -\frac{1}{T_g}\int_0^{T_g} (Z_0^{(g)}(s+\Delta))^T \left.\frac{\partial G(\gamma_g(s+\Delta;0),\gamma_f(s;0,0);\delta)}{\partial \delta}\right|_{\delta=0} ds
\end{aligned}
\tag{3.58}
$$

exactly as in the proof of Lemma 3.6.

Step 2: Let $\beta \to \beta^*$ and keep $\delta = \delta^*$ fixed to reintroduce the timing discrepancy in the oscillators (point 3 $\to$ point 4 in Fig. 3.3). By assumption, when $\beta = \beta^*$ and $\delta = \delta^*$ (coupled oscillators with non-identical periods), system (3.56) admits a unique linearly asymptotically stable 1:1 mode-locked solution, $\gamma(t;\delta^*,\beta^*) = \gamma(t+\mathcal{T}^*;\delta^*,\beta^*)$. Furthermore, when $\beta = 0$ and $\delta = \delta^*$ (stable limit cycle corresponding to a stable 1:1 mode-locked solution), by Lemma 3.2, (3.56) admits a well-defined $\mathcal{T}$-periodic iSRC, $\Gamma_1(t)$ corresponding to $\gamma(t;\delta^*,\beta^*)$, which satisfies

$$
\begin{aligned}
\Gamma_1'(t) &= \begin{bmatrix} D\tilde{F}_x(\gamma_f(t;\delta^*,0),\gamma_g(t;\delta^*,0);\delta,0)) & D\tilde{F}_y(\gamma_f(t;\delta^*,0),\gamma_g(t;\delta^*,0);\delta,0)) \\ DG_x(\gamma_g(t;\delta^*,0),\gamma_f(t;\delta^*,0);\delta)) & DG_y(\gamma_g(t;\delta^*,0),\gamma_f(t;\delta^*,0);\delta)) \end{bmatrix} \Gamma_1(t) \\
&\quad + \nu_1 \begin{bmatrix} \tilde{F}(\gamma_f(t;\delta^*,0),\gamma_g(t;\delta^*,0);\delta,0) \\ G(\gamma_g(t;\delta^*,0),\gamma_f(t;\delta^*,0);\delta) \end{bmatrix} + \left.\begin{bmatrix} \frac{\partial \tilde{F}(\gamma_f(t;\delta^*,0),\gamma_g(t;\delta^*,0);\delta,\beta)}{\partial \beta} \\ 0 \end{bmatrix}\right|_{\beta=0}
\end{aligned}
\tag{3.59}
$$

with linear shift in frequency given by

$$\nu_1 = -\frac{1}{\mathcal{T}} \int_0^{\mathcal{T}} (Z_0(s))^T \left[\begin{matrix} \frac{\partial \tilde{F}(\gamma_f(t;\delta^*,0),\gamma_g(t;\delta^*,0);\delta,\beta)}{\partial \beta} \\ 0 \end{matrix} \right] \Bigg|_{\beta=0} ds \tag{3.60}$$

where $Z_0(t)$ is the iPRC corresponding to $\gamma(t;\delta^*,0)$.

Without loss of generality, introduce frequency constants η_j, $j = 1, \ldots, 4$, so that $\gamma_f(\eta_1 t; 0, \beta^*)$, $\Gamma_1(\eta_2 t)$, $\gamma(\eta_3 t, \delta^*, 0)$ and $\gamma(\eta_4 t, \delta^*, \beta^*)$ are T_g-periodic. These time scalings are introduced so that a pointwise comparison of the unperturbed and perturbed orbits via the iSRC can be performed in a consistent manner (as in (2.15)) and have no influence on the shape of the curves. Then, by the computations in steps 1 and 2,

$$\gamma(\eta_3 t, \delta^*, 0) = \begin{bmatrix} \gamma_f(\eta_1 t; 0, \beta^*) \\ \gamma_g(t; 0) \end{bmatrix} + \delta \Upsilon_1(t) + \mathcal{O}(\delta^2) \tag{3.61}$$

and

$$\gamma(\eta_4 t; \delta^*, \beta^*) = \gamma(\eta_3 t; \delta^*, 0) + \beta \Gamma_1(\eta_2 t) + \mathcal{O}(\beta^2) \tag{3.62}$$

It follows that

$$\underbrace{\gamma(\eta_4 t; \delta^*, \beta^*)}_{\text{perturbed orbit}} = \underbrace{\begin{bmatrix} \gamma_f(\eta_1 t; 0, \beta^*) \\ \gamma_g(t; 0) \end{bmatrix}}_{\text{unperturbed orbit}} + \underbrace{\delta \Upsilon_1(t) + \beta \Gamma_1(\eta_2 t)}_{\text{iSRC}} + \mathcal{O}(\delta^2) + \mathcal{O}(\beta^2) \tag{3.63}$$

so that the iSRC for the original system (3.55) is given by a linear combination of two iSRCs: one corresponding to the coupling (step 1) and the other corresponding to the timing discrepancy (step 2). ∎

Adding the two iSRCs as in (3.63) is valid provided that an appropriate base point on the intermediate orbit, $\gamma(t;\delta^*,0)$, is chosen. The iSRC establishes a pointwise correspondence between unperturbed and perturbed (coupled) orbits. The Poincaré section chosen in step 1 establishes such a correspondence between the base point on the unperturbed orbit, $\gamma(t;0,0)$, and the intersection point of that section with the intermediate orbit, $\gamma(t;\delta^*,0)$. A different section chosen in step 2 establishes a correspondence between the base point on $\gamma(t;\delta^*,0)$ and the intersection point of this other section with the perturbed orbit, $\gamma(t;\delta^*,\beta^*)$. One way to guarantee that (3.63) holds, i.e., that the base point on the unperturbed orbit is mapped to the intersection point on the final perturbed orbit, is to choose the intersection point on $\gamma(t;\delta^*,0)$ from step 1 as the base point on $\gamma(t;\delta^*,0)$ from step 2.

3.4. Tracking Extrema of State Variables. Previous work demonstrated that the iSRC is useful for tracking how the average value of specific system observables changes as a parameter is varied [77]. Here, we establish a new result, that complements the existing theory, by deriving an iSRC-based method to track the *extrema* of specific system states. Tracking oscillation extrema is particularly useful for systems with dynamics that change drastically once a certain ‘threshold’ value is met. Examples include cellular apoptosis [51], stochastic resonance [18], periodically forced integrate-and-fire neurons [10, 11], motor control systems [21, 39, 68], and the role of glucose oscillations in diabetes [40].

Recall that the iSRC establishes a pointwise correspondence between unperturbed and perturbed limit-cycle orbits. By Lemma 2.3 in [67], a particular iSRC (specified by a particular choice of Poincaré section) is a member of a vector equivalence class. Consequently, it is not true in general that the extrema of the unperturbed limit cycle will have a pointwise correspondence via the iSRC to the extrema of the perturbed limit cycle. Such a direct correspondence would obtain only for certain choices of Poincaré section. In such cases, one could add the iSRC to the unperturbed limit cycle to obtain an approximation for the position of the extremum. To address the general case, we show how one can determine the point on the unperturbed limit cycle that maps to an extremum on the perturbed limit cycle, for arbitrary choice of section, by determining an appropriate phase offset. Without loss of generality, we consider a maximal value of some component of the limit cycle trajectory; the case of a minimum can be handled *mutatis mutandis*.

LEMMA 3.8. *Consider a system of the form*

$$\mathbf{x}'(t;\epsilon) = F(\mathbf{x};\epsilon) = f(\mathbf{x}) + \epsilon \cdot u(\mathbf{x}) \tag{3.64}$$

which satisfies the single oscillator iSRC assumptions (B1-B3). Fix a component of interest $\gamma \cdot \vec{e}_i$ for some $i \in \{1, 2, \dots, n\}$, where $\vec{e}_i$ represents the canonical basis vector. Assume that for this i, $\gamma''(t;0)$ exists and that $\gamma(t;0)\cdot\vec{e}_i$ has a well-defined maximum at time t_m in the sense that $\gamma''(t_m;0)\cdot\vec{e}_i \neq 0$. Then, the value of this maximum may be tracked in the perturbed system to linear order in ϵ by

$$\max(\gamma(t;\epsilon)\cdot\vec{e}_i) = \left[\gamma(t_m+\epsilon\Xi^*;0) + \epsilon\gamma_1(t_m+\epsilon\Xi^*)\right]\cdot\vec{e}_i + \mathcal{O}(\epsilon^2) \tag{3.65}$$

where the appropriate phase shift, Ξ^*, corresponding to an infinitesimal perturbation, is given by

$$\Xi^* = -\frac{\left(Df(\gamma(t_m;0))\gamma_1(t_m) + \left.\frac{\partial F(\gamma(t_m;0);\epsilon)}{\partial\epsilon}\right|_{\epsilon=0}\right)\cdot\vec{e}_i}{Df(\gamma(t_m;0))f(\gamma(t_m;0))\cdot\vec{e}_i} \tag{3.66}$$

Proof. We seek to maximize the quantity

$$\left[\gamma(t_m+\epsilon\Xi;0) + \epsilon\gamma_1(t_m+\epsilon\Xi)\right]\cdot\vec{e}_i \tag{3.67}$$

by finding the optimal value of the phase-shift, Ξ. To solve for Ξ, we expand, then differentiate

$$\begin{aligned} 0 &= \frac{\partial}{\partial\Xi}\left[\gamma(t+\epsilon\Xi;0) + \epsilon\gamma_1(t+\epsilon\Xi)\right]\cdot\vec{e}_i \\ &= \frac{\partial}{\partial\Xi}\Bigg[\gamma(t;0) + \epsilon\Xi\gamma'(t;0) + \frac{1}{2}\epsilon^2\Xi^2\gamma''(t;0) \\ &\qquad + \epsilon\left(\gamma_1(t) + \epsilon\Xi\gamma_1'(t) + \frac{1}{2}\epsilon^2\Xi^2\gamma_1''(t)\right) + \mathcal{O}(\Xi^3)\Bigg]\cdot\vec{e}_i \\ &= \left[\epsilon\gamma'(t;0) + \epsilon^2\Xi\gamma''(t;0) + \epsilon\Big(\epsilon\gamma_1'(t) + \epsilon^2\Xi\gamma_1''(t)\Big) + \mathcal{O}(\Xi^2)\right]\cdot\vec{e}_i \end{aligned} \tag{3.68}$$

Disregarding higher order terms, evaluating at $t = t_m$, and solving for $\epsilon\Xi$ gives

$$\epsilon\Xi = -\frac{\Big(\gamma'(t_m;0) + \epsilon\gamma_1'(t_m)\Big)\cdot\vec{e}_i}{\Big(\gamma''(t_m;0) + \epsilon\gamma_1''(t_m)\Big)\cdot\vec{e}_i} \tag{3.69}$$

Observe that $\gamma'(t_m;0) = f(\gamma(t_m;0))$ and further that $f(\gamma(t_m;0))\cdot\vec{e}_i = 0$ because the ith component of the vector field is necessarily zero at $t = t_m$. Therefore,

$$\epsilon\Xi = -\frac{\Big(\epsilon\gamma_1'(t_m)\Big)\cdot\vec{e}_i}{\Big(\gamma''(t_m;0) + \epsilon\gamma_1''(t_m)\Big)\cdot\vec{e}_i} \tag{3.70}$$

which implies that

$$\Xi = -\frac{\Big(\gamma_1'(t_m)\Big)\cdot\vec{e}_i}{\Big(\gamma''(t_m;0) + \epsilon\gamma_1''(t_m)\Big)\cdot\vec{e}_i} \tag{3.71}$$

Taking the limit as $\epsilon \to 0$ gives a formula for the infinitesimal phase-shift, Ξ^*, of the locus of the maximum

$$\Xi^* = -\frac{\gamma_1'(t_m)\cdot\vec{e}_i}{\gamma''(t_m;0)\cdot\vec{e}_i} \tag{3.72}$$

with convergence guaranteed by the assumption that $\gamma''(t_m;0)\cdot\vec{e}_i \neq 0$. Observe that this relation can be expressed using only knowledge of the base system and the iSRC

$$\Xi^* = -\frac{\left(Df(\gamma(t_m;0))\gamma_1(t_m) + \frac{\partial F(\gamma(t_m;0);\epsilon)}{\partial\epsilon}\bigg|_{\epsilon=0}\right)\cdot\vec{e}_i}{Df(\gamma(t_m;0))f(\gamma(t_m;0))\cdot\vec{e}_i} \tag{3.73}$$ ∎

We now show that our expression accounts for an arbitrary choice of Poincaré section. Indeed, note that the rate of change of the maximum as a function of ϵ is

$$\begin{aligned}
&\frac{d}{d\epsilon}\left[\gamma(t_m + \epsilon\Xi^*;0) + \epsilon\gamma_1(t_m + \epsilon\Xi^*)\right]\cdot\vec{e}_i \\
&\quad = \frac{d}{d\epsilon}\left[\gamma(t_m;0) + \epsilon\Xi^*\gamma'(t_m;0) + \mathcal{O}(\epsilon^2) + \epsilon\Big(\gamma_1(t_m) + \epsilon\Xi^*\gamma_1'(t_m) + \mathcal{O}(\epsilon^2)\Big)\right]\cdot\vec{e}_i \\
&\quad = \Big[\Xi^*\gamma'(t_m;0) + \gamma_1(t_m)\Big]\cdot\vec{e}_i + \mathcal{O}(\epsilon)
\end{aligned} \tag{3.74}$$

Disregarding higher order terms, the rate of change (RoC) of the locus of the maximum in $\mathbb{R}^n$ satisfies

$$\text{RoC of Maximal Point} = \Xi^* f(\gamma(t_m;0)) + \gamma_1(t_m) \tag{3.75}$$

The expression (3.75) is the $\mathcal{O}(\epsilon)$ term in an expansion for the true location of the maximum. If a (reference) Poincaré section is chosen so that the maximum on the unperturbed limit cycle is mapped to the corresponding maximum on the perturbed limit cycle, then $\Xi^* = 0$ and we obtain the perturbed maximum by adding the iSRC. Otherwise, we may compare the Poincaré section which was chosen with the previous (reference) section. By Lemma 2.3 in [67], each of these choices results in two distinct iSRCs, which are related in that their difference is given by a constant scaling of the unperturbed vector field: the first term in (3.75). That is, the effect of choosing a different Poincaré section (choosing a different normal vector $\vec{n}$) is equivalent to keeping $\vec{n}$ fixed while simultaneously introducing a phase-shift scaling the unperturbed vector field. Note that Ξ^* is a function of $\vec{n}$ by its dependence on the iSRC, $\gamma_1(t)$. This representation makes it clear that to linear order in ϵ, the shift in the locus of the maximum is given by a linear combination of the iSRC and a scaled vector field which accounts for the arbitrary choice of Poincaré section.

3.5. Higher Order iSRC Terms. The iSRC analysis holds to only linear order in the perturbation strength, and hence loses accuracy when large perturbations are considered. Here, we derive equations for higher order iSRC correction terms. We proceed by following the proof of Lemma 3.2. The computations are straightforward, yet it quickly becomes cumbersome to take the required higher order derivatives. To that end, we adopt notation previously used in [22] to express the required derivatives.

Let P be the set of all partitions of $\{1, 2, \ldots, n\}$. A *partition* of a set A is a grouping of its elements into non-empty subsets so that each $a \in A$ is included in exactly one subset. For example,

$$n = 3 \quad \Longrightarrow \quad P = \{123,\ 12|3,\ 13|2,\ 23|1,\ 1|2|3\} \tag{3.76}$$

where the notation 12|3, for instance, is meant to represent the partition $\{\{1, 2\}, \{3\}\}$. The sets in each partition are *blocks*. For example, the partition 12|3 has two blocks, while the partition 123 has one block.

Consider a composite function $(f \circ g)(x) = f(g(x))$, with $x \in \mathbb{R}$. Following [22], the nth derivative of $f(g(x))$ can be expressed as

$$\frac{d^n}{dx^n} f(g(x)) = \sum_{p \in P} f^{(|p|)}(g(x)) \cdot \prod_{B \in p} g^{(|B|)}(x) \tag{3.77}$$

where the notation $p \in P$ is understood in the sense that p is an index which runs through each partition of P, and the notation $|p|$ represents the number of blocks in that partition. Analogously, the notation $B \in p$ is understood in the sense that B is an index which runs through each block of the partition p, and the notation $|B|$ represents the size of each block. For the sake of clarity, writing out (3.77) explicitly when $n = 3$ gives

(3.78)

$$\begin{aligned}\frac{d^3}{dx^3} f(g(x)) &= f^{(1)}g^{(3)} + f^{(2)}g^{(2)}g^{(1)} + f^{(2)}g^{(2)}g^{(1)} + f^{(2)}g^{(2)}g^{(1)} + f^{(3)}g^{(1)}g^{(1)}g^{(1)} \\ &= f^{(1)}g^{(3)} + 3f^{(2)}g^{(2)}g^{(1)} + f^{(3)}(g^{(1)})^3\end{aligned}$$

where the notation $h^{(j)}$ is the jth derivative of a function h with respect to x. We now derive an expression for the nth order iSRC correction.

LEMMA 3.9. *Consider a system of the form*

$$\mathbf{x}'(t; \epsilon) = F(\mathbf{x}; \epsilon) = f(\mathbf{x}) + \epsilon \cdot u(\mathbf{x}) \tag{3.79}$$

with $\mathbf{x} \in \mathbb{R}^N$ that satisfies the high-order iSRC assumptions:

- *(E1) There exists an open subset* $\Omega \subset \mathbb{R}^N$ *and an open neighborhood of zero* $\mathcal{I} \subset \mathbb{R}$ *such that the vector field* $F(\mathbf{x};\epsilon) : \Omega \times \mathcal{I} \to \mathbb{R}^N$ *is* $\mathcal{C}^n$ *in both the coordinates* $\mathbf{x} \in \Omega$*, and the perturbation strength* $\epsilon \in \mathcal{I}$.
- *(E2) For* $\epsilon \in \mathcal{I}$*, the system (3.79) admits a linearly asymptotically stable* $T(\epsilon)$*-periodic limit cycle* $\gamma(t;\epsilon) \in \Omega$*, where* $T(\epsilon)$ *has* $\mathcal{C}^n$ *dependence on* ϵ.

Then, system (3.79) admits an nth order iSRC expansion of the form

$$\begin{aligned} \gamma(\tau(t);\epsilon) &= \gamma(t;0) + \epsilon\gamma_1(t) + \epsilon^2\gamma_2(t) + \cdots + \epsilon^n\gamma_n(t) \quad \textit{(uniformly in } t\textit{)} \\ \tau(t) &= t(1 - \epsilon\nu_1 - \epsilon^2\nu_2 - \cdots - \epsilon^n\nu_n) \end{aligned} \tag{3.80}$$

where the formula for $\gamma_k = \gamma_k(t)$ *with* $2 \le k \le n$ *is given by*

$$\begin{aligned} \gamma_k' = Df\gamma_k + \left[\nu_k f + \sum_{j=1}^{k-1} \nu_j \gamma_{k-j}'\right] + \frac{1}{k!}\left[\sum_{p\in P^*} f^{(|p|)} \cdot \prod_{B\in p} |B|!\gamma_{|B|}\right] \\ + \frac{1}{(k-1)!}\left[\sum_{q\in Q} (\partial_\epsilon F)^{(|q|)} \cdot \prod_{C\in q} |C|!\gamma_{|C|}\right] \end{aligned} \tag{3.81}$$

with

$$\begin{aligned} \nu_k = -\frac{1}{T}\int_0^T (Z_0(t))^T \Bigg(\sum_{j=1}^{k-1} \nu_j\gamma_{k-j}' + \frac{1}{k!}\left[\sum_{p\in P^*} f^{(|p|)} \cdot \prod_{B\in p} |B|!\gamma_{|B|}\right] \\ + \frac{1}{(k-1)!}\left[\sum_{q\in Q} (\partial_\epsilon F)^{(|q|)} \cdot \prod_{C\in q} |C|!\gamma_{|C|}\right]\Bigg) dt \end{aligned} \tag{3.82}$$

The vector field f*, the Jacobian* $Df = \frac{\partial f}{\partial x}$*, the derivatives* $f^{(|p|)} = \frac{\partial^{|p|} f}{\partial x^{|p|}}$*, and the derivatives* $(\partial_\epsilon F)^{(|q|)} = \frac{\partial^{|q|+1} f}{\partial \epsilon \partial x^{|q|}}$ *are evaluated at* $\gamma(t;0)$*. Here,* $P^* = P \setminus \{\{1,2,\ldots,k\}\}$ *and* Q *is the set of all permutations of* $\{1,2,\ldots,k-1\}$.

A detailed proof of Lemma 3.9 is provided in Appendix C in the supplementary materials. We remark that the initial condition for (3.81) describing the dynamics of a single oscillator is computed as described in the earlier Lemma 3.4. The only difference is that the inhomogeneous term in the nth order equation changes, i.e., the $b(t)$ term from the proof of Lemma 3.4 changes. This formalism also applies to the computation of an iSRC corresponding to coupled oscillators with identical periods, as in §3.2. In this case, one arrives at a different frequency matching condition for each higher order correction. In practice, therefore, a different choice of base point for each γ_j is required. To ensure that one can add the higher order corrections in a consistent manner, a different Poincaré section must be chosen for each γ_j to maintain the pointwise correspondence established by the original choice of section for γ_1.

The higher order iSRC equations must be computed in order, starting with $n = 1$. We note that our closed form expression becomes impractical after $n = 4$ or $n = 5$ because the cardinality of P^* becomes quite large. For convenience, we provide the formula for the iSRC corrections to third order in ϵ

(3.83)

$$
\begin{aligned}
\gamma_1' &= Df(\gamma_0)\gamma_1 + \nu_1 f(\gamma_0) + \left.\frac{\partial F(\gamma_0;\epsilon)}{\partial \epsilon}\right|_{\epsilon=0} \\
\gamma_2' &= Df(\gamma_0)\gamma_2 + \left[\nu_1\gamma_1' + \nu_2 f(\gamma_0)\right] + \frac{1}{2}\frac{\partial^2 f(\gamma_0)}{\partial x^2}(\gamma_1)^2 + \left.\frac{\partial^2 F(\gamma_0;\epsilon)}{\partial x \partial \epsilon}\right|_{\epsilon=0}(\gamma_1) \\
\gamma_3' &= Df(\gamma_0)\gamma_3 + \left[\nu_1\gamma_2' + \nu_2\gamma_1' + \nu_3 f(\gamma_0)\right] + \frac{1}{6}\frac{\partial^3 f(\gamma_0)}{\partial x^3}(\gamma_1)^3 + \frac{\partial^2 f(\gamma_0)}{\partial x^2}(\gamma_1\gamma_2) \\
&\quad + \left.\frac{\partial^2 F(\gamma_0;\epsilon)}{\partial x \partial \epsilon}\right|_{\epsilon=0}(\gamma_2) + \frac{1}{2}\left.\frac{\partial^3 F(\gamma_0;\epsilon)}{\partial x^2 \partial \epsilon}\right|_{\epsilon=0}(\gamma_1)^2
\end{aligned}
$$

To understand the notation used in these equations, we review formalism presented in [72]. Let $f(\gamma_0) = \begin{bmatrix} f_1(\gamma_0) & \dots & f_N(\gamma_0) \end{bmatrix}^T$, where T denotes the matrix transpose, and let $f_j^{(0)} = f_j(\gamma_0)$. Define a sequence of matrices for $i \geq 1$

$$f_j^{(i)}(\gamma_0) = \frac{\partial \mathrm{vec}(f_j^{(i-1)}(\gamma_0))}{\partial x^T} \in \mathbb{R}^{N^{i-1}\times N} \tag{3.84}$$

where $\mathrm{vec}(\cdot)$ is the vectorization operator which stacks the columns of a matrix on top of each other. In words, $f_j^{(i)}(\gamma_0)$ is computed by vectorizing $f_j^{(i-1)}(\gamma_0)$, then taking the Jacobian. See Appendix F for an example computation of (3.84). This notation allows for a convenient representation of the Taylor expansion of $f(\gamma_0)$, say about a small perturbation $d\mathbf{x}$

$$f(\gamma_0 + d\mathbf{x}) = f(\gamma_0) + Df(\gamma_0)d\mathbf{x} + \begin{bmatrix} \sum_{i=2}^{\infty} \frac{1}{i!}[\otimes^i (d\mathbf{x})^T]\mathrm{vec}(f_1^{(i)}(\gamma_0)) \\ \vdots \\ \sum_{i=2}^{\infty} \frac{1}{i!}[\otimes^i (d\mathbf{x})^T]\mathrm{vec}(f_N^{(i)}(\gamma_0)) \end{bmatrix} \tag{3.85}$$

where $\otimes$ is the Kronecker product and, as an example, the superscript is understood to represent

$$[\otimes^4 (d\mathbf{x})^T] = (d\mathbf{x})^T \otimes (d\mathbf{x})^T \otimes (d\mathbf{x})^T \otimes (d\mathbf{x})^T \tag{3.86}$$

This formalism easily extends to the representation of the higher order derivatives in (3.83). For example,

$$
\begin{aligned}
\frac{\partial^2 f(\gamma_0)}{\partial x^2}(\gamma_1)^2 &= \begin{bmatrix} [\otimes^2(\gamma_1)^T]\mathrm{vec}(f_1^{(2)}(\gamma_0)) \\ \vdots \\ [\otimes^2(\gamma_1)^T]\mathrm{vec}(f_N^{(2)}(\gamma_0)) \end{bmatrix} \\
\frac{\partial^2 f(\gamma_0)}{\partial x^2}(\gamma_1\gamma_2) &= \begin{bmatrix} [(\gamma_1)^T \otimes (\gamma_2)^T]\mathrm{vec}(f_1^{(2)}(\gamma_0)) \\ \vdots \\ [(\gamma_1)^T \otimes (\gamma_2)^T]\mathrm{vec}(f_N^{(2)}(\gamma_0)) \end{bmatrix}
\end{aligned}
\tag{3.87}
$$

and so forth.

We illustrate our results by computing the iSRC terms up to fourth order for

$$x' = x - x^3 - y + \epsilon x \tag{3.88}$$
$$y' = x + \epsilon y$$

where $\epsilon = 0.3$ (see Figure 3.4).

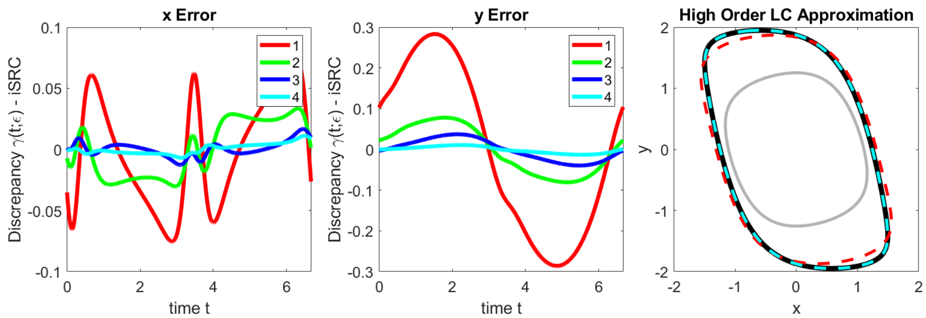

FIGURE 3.4. *Higher order terms can improve the accuracy of the iSRC approximation.* ***Left:*** *The difference between the true perturbed solution $\gamma(t;\epsilon)$ and the iSRC approximation of orders 1 to 4 (red, green, blue, light blue, respectively). The 4th order approximation is significantly more accurate than the 1st order.* ***Right:*** *The unperturbed limit cycle, $\gamma(t;0)$ (light gray), overlayed with the true perturbed solution, $\gamma(t;\epsilon)$ (black), and the 1st (red) and 4th (light blue) iSRC approximations. Despite the large shape change, the 4th order iSRC approximation is still accurate.*

4. Applications.

4.1. Supercritical Hopf Normal Form. As a pedagogical example, we compute the iSRC for the normal form of a supercritical hopf bifurcation in two dimensions

$$x' = (\mu - x^2 - y^2)x - \omega y \tag{4.1}$$
$$y' = (\mu - x^2 - y^2)y + \omega x$$

For $\mu > 0$, the system admits a periodic solution in the form of a circle

$$x = \sqrt{\mu}\cos(\omega t), \quad y = \sqrt{\mu}\sin(\omega t) \tag{4.2}$$

The amplitude (maximum of the state variables) of this orbit grows as $\sqrt{\mu}$. We provide analytic solutions for the iSRC in Cartesian, polar, and phase-amplitude coordinates.

Suppose that $\omega = 1$ is fixed. Let $\mu_0 > 0$ represent the unperturbed system amplitude and let ϵ be a small, variable parameter. Let the system amplitude, μ, vary by writing $\mu = \mu_0 + \epsilon$ so that the system becomes

$$x' = (\mu_0 + \epsilon - x^2 - y^2)x - y \tag{4.3}$$
$$y' = (\mu_0 + \epsilon - x^2 - y^2)y + x$$

With initial condition $\mathbf{x}_0 = (\sqrt{\mu_0}, 0)$ and Poincaré section spanned by $(1, 0)$ so that the relative phase difference between the unperturbed and perturbed systems is zero, one can verify by direct computation (solving (2.13), (2.14), and (3.21)) that the iSRC is given by (see Appendix G for further details)

$$\gamma_1(t) = \frac{1}{2\sqrt{\mu_0}}\begin{bmatrix}\cos(t)\\ \sin(t)\end{bmatrix} \tag{4.4}$$

By (2.15), the iSRC predicts that the perturbed trajectory will be of the form

$$\gamma_\epsilon(t) = \sqrt{\mu_0}\begin{bmatrix}\cos(t)\\ \sin(t)\end{bmatrix} + \epsilon\frac{1}{2\sqrt{\mu_0}}\begin{bmatrix}\cos(t)\\ \sin(t)\end{bmatrix} = \left(\sqrt{\mu_0} + \epsilon\frac{1}{2\sqrt{\mu_0}}\right)\begin{bmatrix}\cos(t)\\ \sin(t)\end{bmatrix} \tag{4.5}$$

and therefore predicts that the amplitude will vary linearly in ϵ with slope $1/(2\sqrt{\mu_0})$. Indeed, note that the rate of change of the system amplitude at μ_0 is given by

$$\frac{d}{d\mu}\sqrt{\mu}\bigg|_{\mu=\mu_0} = \frac{1}{2\sqrt{\mu_0}} \tag{4.6}$$

and so the iSRC behaves as it should by giving the amplitude change to linear order in ϵ (see Figure 4.1).

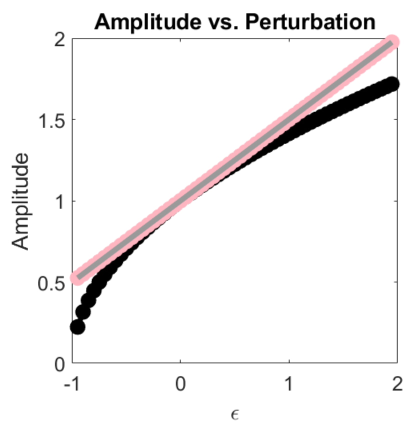

FIGURE 4.1. *The amplitude of the Hopf normal form system (4.3) as a function of the perturbation ϵ with $\mu_0 = \omega = 1$. The true system amplitude (black) goes as $\sqrt{\mu}$. The amplitude predicted by the iSRC (pink) matches the slope of the tangent line to $\sqrt{\mu}$ at μ_0 (gray).*

In polar coordinates, (4.3) becomes

$$\begin{aligned}\theta' &= 1\\ r' &= (\mu_0 + \epsilon - r^2)r\end{aligned} \tag{4.7}$$

By writing the iSRC equation (2.13) using the polar representation (4.7), one can directly solve the resulting system and verify that the iSRC is given by

$$\gamma_1(t) = \begin{bmatrix}0\\ \frac{1}{2\sqrt{\mu_0}}\end{bmatrix} \tag{4.8}$$

Direct comparison of equations (4.4) and (4.8) reveals their equivalence. In both cases, there is no phase shift and the radius increases linearly with respect to ϵ with rate given by $1/(2\sqrt{\mu_0})$.

Finally, we compute the iSRC in phase-amplitude coordinates. One can verify directly that the iPRC and iIRC for the system are given by

$$Z_0 = \frac{1}{\sqrt{\mu_0}}\begin{bmatrix}-\sin(t)\\ \cos(t)\end{bmatrix}, \quad I_0 = \frac{1}{\alpha}\begin{bmatrix}\cos(t)\\ \sin(t)\end{bmatrix} \tag{4.9}$$

where the constant α corresponds to the arbitrary scaling constant used in the computation of the $\mathbf{K}$ function in the parameterization method [49]. The iIRC is scaled by an arbitrary constant because the amplitude coordinates are defined up to an arbitrary multiplicative constant. By substituting these expressions into the iSRC equation, one may directly verify that the iSRC, in phase-amplitude coordinates, is given by

$$\gamma_1(t) = \begin{bmatrix} 0 \\ \frac{1}{2\alpha\sqrt{\mu_0}} \end{bmatrix} \tag{4.10}$$

Note the similarity in structure of the iSRC in polar coordinates and in amplitude coordinates. The phase component of the iSRC is identical in both coordinate systems. One can verify that the isochrons (level curves of the phase function) of (4.1) are evenly spaced spokes of a wheel. Thus, in this simple example the polar phase variable is identical to the phase variable in isostable coordinates. The radial/amplitude component have similar structures, but are not identical due to the arbitrary multiplicative scaling associated with the amplitude coordinate.

4.2. Coupled Oscillators with Identical Periods. Systems of coupled Van der Pol oscillators are commonly used as simple mathematical models to describe physically important phenomena, such as circadian rhythms [53], heart rhythms and pacemakers [55], and locomotion [36, 38]. It is desirable to understand how the shape of such oscillations are influenced by sustained perturbations, e.g., changes in the environment. Here, we demonstrate that our joint phase-amplitude iSRC approach may be effectively applied to systems of this form. We consider coupling structures corresponding to both entrainment and synchronization. In each case, we consider two non-identical Van der Pol oscillators given by

$$\begin{aligned} x' &= \mathcal{T}\,(x - x^3 - y) \\ y' &= \mathcal{T}\,x \end{aligned} \tag{4.11}$$

and

$$\begin{aligned} w' &= w - w^3 - z + \epsilon \\ z' &= w + \epsilon \end{aligned} \tag{4.12}$$

where $\mathcal{T} = T_x/T_w$ is the ratio of the natural period of the first (T_x) and second (T_w) oscillators. Multiplying the dynamics of the first oscillator by the ratio of the periods ensures that each oscillator has period T_w, yet does not change the shape of the first oscillator. Here, $\epsilon = 0.1$ is fixed so that oscillator 2 admits a limit-cycle solution that has slightly perturbed shape in comparison with that of oscillator 1. Note that each of oscillators 1 and 2 satisfy assumptions (A1-A3) and thus admit well-defined phase-amplitude reductions via the parameterization method.

4.2.1. Entrainment. We consider a coupled system of the form

$$\begin{aligned} x' &= \mathcal{T}\,(x - x^3 - y) + \delta(w - x) \\ y' &= \mathcal{T}\,x \\ w' &= w - w^3 - z + \epsilon \\ z' &= w + \epsilon \end{aligned} \tag{4.13}$$

where $\delta = -0.03$. Note that this system is of the form (3.32) with $u_g = 0$. We apply Lemma 3.6 to compute the iSRC of (4.13) in phase-amplitude coordinates.

Appendix D in the supplementary materials demonstrates that assumptions (D1-D4) pertaining to Lemma 3.6 are satisfied, both for $\delta < 0$ (anti-synchronous) and for $\delta > 0$ (synchronous). We find numerically that the system admits a unique linearly asymptotically stable 1:1 mode locked solution with the oscillations of the two systems in anti-synchrony. The dynamics of oscillator 2 are not affected by the coupling; this model corresponds to a scenario in which oscillator 2 entrains oscillator 1.

In the 1:1 mode locked solution of (4.13), the orbit of oscillator 1 is distorted when $\delta \neq 0$, but the orbit of oscillator 2 is unaffected by the perturbation. We combine phase-amplitude reduction and the iSRC to analyze the shape change of oscillator 1 under entrainment. Recall that by Lemma 3.6, it is necessary only to implement phase-amplitude reduction and compute the iSRC for each uncoupled system. In the case of entrainment, we need only compute the iSRC for oscillator 1, as the dynamics of oscillator 2 remain unchanged. To gauge the numerical accuracy of the iSRC, we compute the relative L_2 norm of the approximation.[1] Figure 4.2 shows the results.

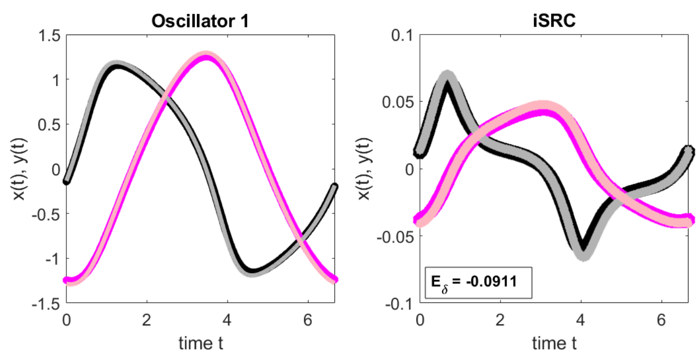

FIGURE 4.2. *Dynamics of the entrained and original Van der Pol systems.* ***Left:*** *The perturbed steady-state trajectories of oscillator 1 ($x(t)$ - gray, and $y(t)$ - light pink) overlayed with its unperturbed trajectories ($x(t)$ - black, and $y(t)$ - pink).* ***Right:*** *The difference between the perturbed and unperturbed trajectories of oscillator 1 ($x(t)$ - black, and $y(t)$ - pink) closely match the iSRC prediction ($x(t)$ - gray, and $y(t)$ - light pink).*

4.2.2. Synchronization. We consider a coupled system of the form

$$\begin{aligned} x' &= \mathcal{T}\,(x - x^3 - y) + \delta(w - x) \\ y' &= \mathcal{T}\,x \\ w' &= w - w^3 - z + \epsilon + \delta(x - w) \\ z' &= w + \epsilon \end{aligned} \tag{4.14}$$

where $\delta = -0.1$. We apply Lemma 3.6 to compute the iSRC of (4.14) in phase-amplitude coordinates. Appendix D in the supplementary materials demonstrates that assumptions (D1-D4) pertaining to Lemma 3.6 are satisfied for both $\delta < 0$ (anti-synchronous) and $\delta > 0$ (synchronous). For this choice of parameters, we find numerically a linearly asymptotically stable 1:1 mode-locked solution with oscillations in anti-synchrony.

The perturbed four-dimensional orbit consists of a slightly perturbed orbit corresponding to oscillator 1 and a slightly perturbed orbit corresponding to oscillator

[1] We define the error as $\mathcal{E}_\delta = (1/\delta)||\gamma(\tau(t);\delta) - \gamma(t,0) - \delta\gamma_1(t)||/||\gamma(\tau(t);\delta) - \int_0^T \gamma(\tau(t);\delta)dt/T||$.

2. We use the iSRC in conjunction with phase-amplitude reduction to characterize the shape change of the orbits of each oscillator. We reiterate that by Lemma 3.6, one need only implement phase-amplitude reduction and compute the iSRC for each individual oscillator separately. Figure 4.3 shows the results.

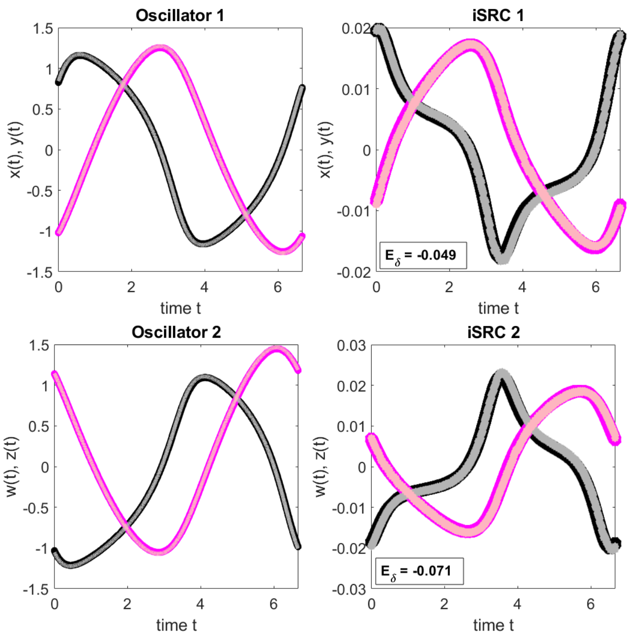

FIGURE 4.3. *Dynamics of the synchronized and original Van der Pol systems. The top row corresponds to oscillator 1, and the bottom to oscillator 2.* ***Left****: the perturbed steady-state trajectories* ($x(t), w(t)$ *- gray, and* $y(t), z(t)$ *- light pink) overlayed with the unperturbed trajectories* ($x(t), w(t)$ *- black, and* $y(t), z(t)$ *- pink).* ***Right****: The difference between the perturbed and unperturbed trajectories* ($x(t), w(t)$ *- black, and* $y(t), z(t)$ *- pink) closely match the iSRC prediction* ($x(t), w(t)$ *- gray, and* $y(t), z(t)$ *- light pink).*

4.3. Coupled Oscillators with Non-Identical Periods. Here, we study the synchronization of a system of two coupled oscillators with different periods. We consider a system consisting of a Stuart-Landau oscillator and a Van der Pol oscillator

$$\begin{aligned} x' &= (\mu - x^2 - y^2)x - \eta y + \delta(w - x) \\ y' &= (\mu - x^2 - y^2)y + \eta x \\ w' &= (1+\beta)(w - w^3 - z) + \delta(x - w) \\ z' &= (1+\beta)w \end{aligned} \tag{4.15}$$

Here $\mu = 0.5$ and $\beta = 0.001$. We take $\eta = \frac{2\pi}{T}$, where $T = 6.6632$ is the natural period of the w, z (Van der Pol) dynamics when $\beta = 0$. Thus, when $\delta = 0$ and $\beta = 0$, the oscillators have the same period T, but when $\delta = 0$ and $\beta \neq 0$, the oscillators have different periods ($T_{\text{SL}} = 6.6632$, $T_{\text{VdP}} = 6.6566$).

We view the uncoupled system as (4.15) with $\beta = 0.001$ and $\delta = 0$, so that the uncoupled oscillators have different periods. We view the true coupled system as (4.15) with $\beta = 0.001$ and $\delta = 0.1$. With these choices of parameters, we find numerically that the system admits a unique linearly asymptotically stable 1:1 mode-locked solution, with period $T_{1:1} = 6.6374$. To compute the iSRC of the fully coupled system, we proceed according to §3.3, noting that the assumptions of Theorem 3.7 are satisfied. For comparison, we first present results for a first order analysis (Figure 4.4, left panel), then we include higher order terms to improve the approximation of the coupling iSRC (Figure 4.4, right panel), as derived in §3.5.

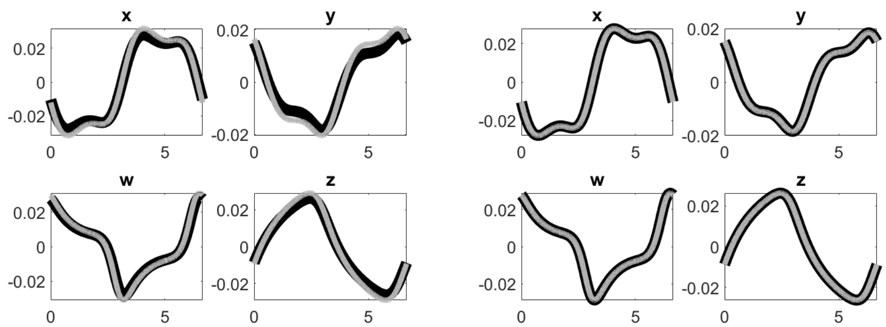

FIGURE 4.4. *Difference of the uncoupled, isoperiodic orbits ($\beta = 0, \delta = 0$) and the fully coupled, anisoperiodic dynamics ($\beta = 0.001, \delta = 0.1$) for the Stuart-Landau / Van der Pol oscillators with unequal frequencies. To allow consistent computation of the difference in the resulting orbits, in both cases the trajectories have been scaled (after coupling, for the latter case) to a common period T_{VdP}. Black: true difference. Gray: iSRC approximation.* ***Left****. 1st order iSRC approximation. The iSRC approximation performs reasonably well.* ***Right****. Here, a 3rd order iSRC was used for the coupling strength computation, and a 1st order iSRC was used for the timing perturbation. The iSRC approximation is excellent.*

4.4. Tracking Extrema of State Variables: Circadian Rhythms. Here, we apply the methods of §3.4 to a two-dimensional model for circadian rhythms describing the oscillation of core body temperature [17, 25]. The model is given by

$$\begin{aligned} x' &= \frac{\pi}{12}\left[y + \mu\left(x - \frac{4x^3}{3}\right) + B\right] \\ y' &= \frac{\pi}{12}\left[-\left(\frac{24}{\tau}\right)^2 x + By\right] \end{aligned} \tag{4.16}$$

where $\mu = 0.13$, $\tau = 24.2$. Here, B is a parameter which represents the influence of light, x represents endogenous core body temperature, and y is an auxiliary variable. We ask how different levels of sustained light exposure influence the amplitude of the circadian rhythm oscillation. Fix $B_0 = 0.1$ as a baseline level of light exposure. Let ϵ be a small, variable parameter and write $B = B_0 + \epsilon$ so that (4.16) becomes

$$\begin{aligned} x' &= \frac{\pi}{12}\left[y + \mu\left(x - \frac{4x^3}{3}\right) + B_0 + \epsilon\right] \\ y' &= \frac{\pi}{12}\left[-\left(\frac{24}{\tau}\right)^2 x + (B_0 + \epsilon)y\right] \end{aligned} \tag{4.17}$$

Note that system (4.17) satisfies the single oscillator iSRC assumptions (B1-B3) and the requirements of Lemma 3.8. When $\epsilon = 0$, the system admits a stable limit-cycle solution with oscillations of $x(t)$ about zero and with a period of approximately 24 hours. We use the iSRC to analyze the change in amplitude (maximum) of the $x(t)$ oscillations as ϵ varies. As shown in Figure 4.5, the iSRC method correctly predicts the sensitivity of the magnitude (the maximum of x) for small perturbations.

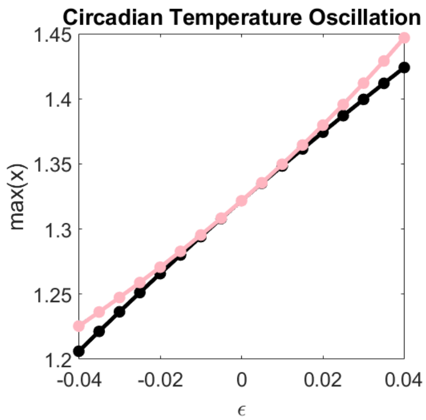

FIGURE 4.5. *The amplitude of the circadian rhythm model as a function of ϵ. The amplitude predicted by the iSRC (pink) agrees well with the true amplitude (black).*

4.5. Non-Planar System. In this section, we demonstrate that our joint iSRC phase-amplitude approach is effective for higher dimensional cases. For concreteness, we study a three-dimensional mean field model for quadratic integrate-and-fire (QIF) neurons subject to a state dependent perturbation [49]. The model equations are specified in Appendix H. We use Theorem 3.1 to compute the iSRC of the QIF model in phase-amplitude coordinates. Results are shown in Figure 4.6.

5. Discussion.

Analysis of the dynamics of weakly perturbed and weakly driven oscillators has been greatly facilitated by the phase-amplitude framework. In phase-amplitude coordinates, highly non-linear oscillatory dynamics are represented in the simplest possible form: a phase variable that evolves at a constant rate, and isostable (amplitude) coordinates that obey linear dynamics. Traditionally, analysis focused solely on the timing of system dynamics [5, 16, 23, 32, 44], and has since been augmented to incorporate a sense of distance from the underlying limit cycle via the introduction of isostable coordinates [7, 20, 73, 74, 75]. Nevertheless, analysis of coupled oscillators is still mainly understood in terms of the timing of the oscillations; for example, a recent study [46] implemented a phase-amplitude reduction to study systems of coupled oscillators, but leveraged knowledge of the amplitude coordinates to arrive at an improved phase-based description of the system dynamics, rather than to study deformations of the trajectory.

Despite the importance of oscillation amplitude in many physical applications, systematic studies on this topic remain lacking. Existing techniques, such as phase-amplitude reduction and the infinitesimal shape response curve, provide a means to study the shape change of weakly perturbed oscillations. However, to the best of our knowledge, no published works have thus far addressed the relation between the iSRC and phase-amplitude methods, or used them in tandem as a joint approach to study oscillation amplitude. In this work, we fill this gap by developing a general framework to study the shape change of perturbed oscillations using a joint iSRC

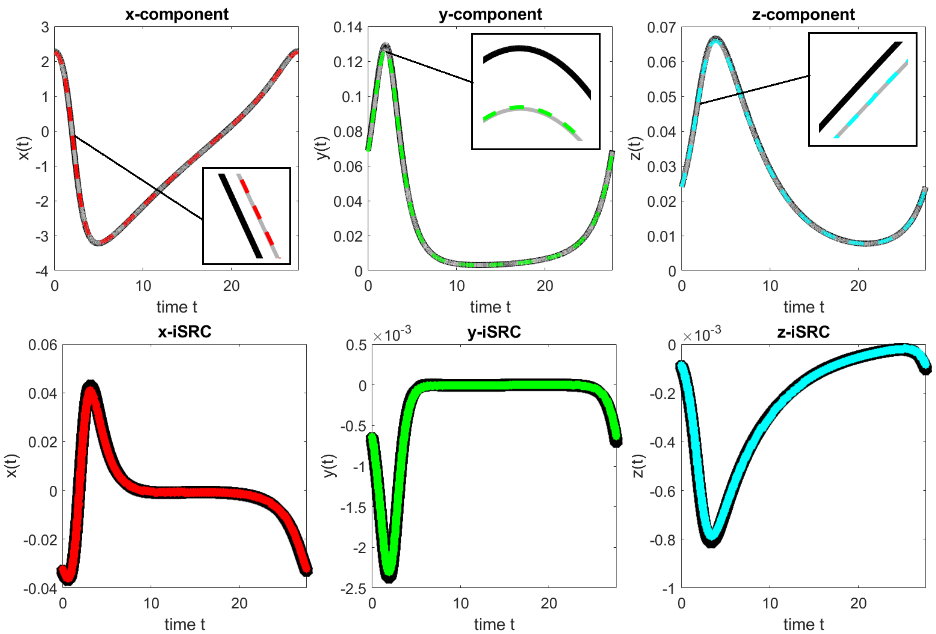

FIGURE 4.6. *Dynamics of the three-dimensional QIF model.* ***Top Row:*** *the unperturbed (black), perturbed (grey), and iSRC approximation (colored) orbits for the x (left), y (middle), and z (right) state variables. The inset is centered at $t = 2.25$.* ***Bottom Row:*** *the difference between the perturbed and unperturbed orbits (black) closely matches the iSRC prediction (x - red, y - green, z - blue).*

phase-amplitude approach.

We specify conditions under which a general class of systems can be analyzed by the iSRC and by phase-amplitude reduction simultaneously. While the iSRC satisfies an ODE which is valid for any coordinate system, we show that potentially highly non-linear iSRC behavior in Cartesian coordinates has a dramatically simple representation in phase-amplitude coordinates. Moreover, by directly relating the iPRC and iIRC to the iSRC, we unify the two methods and demonstrate that our joint approach offers greater conceptual clarity than either of the methods in isolation. In particular, the iPRC and iIRC completely characterize the influence of an arbitrary static perturbation on the shape change of stable limit-cycle dynamics.

In addition to its conceptual importance, we show that the iSRC also leads to practical tools. We use the iSRC in conjunction with phase-amplitude reduction to analyze the synchronization and entrainment of systems of coupled oscillators. In the case of identical periods, we illustrate that one need only analyze each individual oscillator. This analysis allows one to implement lower dimensional phase-amplitude reductions to study high dimensional systems, which can significantly facilitate numerical computation. Previous work [77] demonstrated how the iSRC may be used to track the *average* of specific system observables in limit-cycle systems subject to parametric perturbation. Here, we complement existing theory by showing how the iSRC may be used to track the *extrema* of system states under perturbation. Despite these advances, some open questions remain.

We demonstrated the effectiveness of the phase-amplitude iSRC theory on two- and three-dimensional oscillators. Theoretically, such analysis is applicable to oscillators of higher dimension. However, from a practical standpoint, the implementation of phase-amplitude reduction in dimensions of four or greater quickly becomes cumbersome. Moreover, the non-resonance condition (A3) is not trivially satisfied in dimensions greater than two. It would be desirable to develop computational methods capable of handling such cases.

We developed iSRC theory to analyze the synchronization and entrainment of two coupled oscillators which admit a 1:1 mode locked solution. Extension of this theory to systems of N coupled oscillators should follow straightforwardly from the analysis presented here, yet remains to be implemented numerically. More interesting is the case of N coupled oscillators which admit a non-trivial $p : q$ mode-locked solution. This behavior is observed in physical systems, such as coupling between respiration and locomotion [3], or in neuron models [10], and is worth pursuing in future works.

The work presented here facilitates analysis of coupled deterministic oscillators. However, physically realistic models often incorporate stochasticity, necessitating the study of systems of noisy coupled oscillators. While the notion of deterministic phase as reviewed in this work is not well-defined for stochastic systems, recently notions of stochastic phase and stochastic isostables have gained traction [6, 47, 48, 50, 57, 66]. Such notions allow for the treatment of stochastic oscillators in much the same manner as their deterministic counterparts; a natural future goal is to leverage notions of stochastic phase and amplitude to understand how the effects of coupling and other sustained perturbations distort both the shape and timing of stochastic oscillators.

Acknowledgments. This work was supported in part by NSF grants DMS-2052109 and DMS-1929284, and by the Oberlin College Department of Mathematics. The authors thank Prof. J. Rubin for suggesting the problem of tracking the extremal values of a limit cycle using the iSRC and Prof. A. Pérez for assistance with the non-planar system example.

References.

[1] Sabra M Abbott, Roneil G Malkani, and Phyllis C Zee. “Circadian Disruption and Human Health: A Bidirectional Relationship”. In: *European Journal of Neuroscience* 51.1 (2020), pp. 567–583.

[2] Ameneh Asgari-Targhi and Elizabeth B Klerman. “Mathematical modeling of circadian rhythms”. In: *Wiley Interdisciplinary Reviews: Systems Biology and Medicine* 11.2 (2019), e1439.

[3] Dennis M Bramble and David R Carrier. “Running and Breathing in Mammals”. In: *Science* 219.4582 (1983), pp. 251–256.

[4] Roger W Brockett. *Finite Dimensional Linear Systems*. SIAM, 2015.

[5] Eric Brown, Jeff Moehlis, and Philip Holmes. “On the Phase Reduction and Response Dynamics of Neural Oscillator Populations”. In: *Neural Computation* 16.4 (2004), pp. 673–715.

[6] Alexander Cao, Benjamin Lindner, and Peter J Thomas. “A Partial Differential Equation for the Mean–Return-Time Phase of Planar Stochastic Oscillators”. In: *SIAM Journal on Applied Mathematics* 80.1 (2020), pp. 422–447.

[7] Oriol Castejón, Antoni Guillamon, and Gemma Huguet. “Phase-amplitude response functions for transient-state stimuli”. In: *The Journal of Mathematical Neuroscience* 3.1 (2013), pp. 1–26.

[8] Roberto Castelli, Jean-Philippe Lessard, and Jason D Mireles James. “Parameterization of Invariant Manifolds for Periodic Orbits I: Efficient Numerics via the Floquet Normal Form”. In: *SIAM Journal on Applied Dynamical Systems* 14.1 (2015), pp. 132–167.

[9] YM Chen and JK Liu. "Uniformly Valid Solution of Limit Cycle of the Duffing–Van der Pol Equation". In: *Mechanics Research Communications* 36.7 (2009), pp. 845–850.
[10] S Coombes and Paul C Bressloff. "Mode locking and Arnold tongues in integrate and fire neural oscillators". In: *Physical Review E* 60.2 (1999), p. 2086.
[11] S Coombes and PC Bressloff. "Erratum: Mode locking and Arnold tongues in integrate-and-fire neural oscillators [Phys. Rev. E 60, 2086 (1999)]". In: *Physical Review E* 63.5 (2001), p. 059901.
[12] Tamer Demiralp et al. "Gamma amplitudes are coupled to theta phase in human EEG during visual perception". In: *International Journal of Psychophysiology* 64.1 (2007), pp. 24–30.
[13] Miles Detrixhe et al. "A Fast Eulerian Approach for Computation of Global Isochrons in High Dimensions". In: *SIAM Journal on Applied Dynamical Systems* 15.3 (2016), pp. 1501–1527.
[14] Luvna Dhawka et al. "Low circadian amplitude and delayed phase are linked to seasonal affective disorder (SAD)". In: *Journal of Affective Disorders Reports* 10 (2022), p. 100395.
[15] Emrah Düzel, Will D Penny, and Neil Burgess. "Brain oscillations and memory". In: *Current Opinion in Neurobiology* 20.2 (2010), pp. 143–149.
[16] Bard Ermentrout and David H Terman. *Mathematical Foundations of Neuroscience*. Vol. 35. Springer, 2010.
[17] Daniel B Forger, Megan E Jewett, and Richard E Kronauer. "A Simpler Model of the Human Circadian Pacemaker". In: *Journal of Biological Rhythms* 14.6 (1999), pp. 533–538.
[18] Luca Gammaitoni et al. "Stochastic resonance". In: *Reviews of modern physics* 70.1 (1998), p. 223.
[19] John Guckenheimer. "Isochrons and phaseless sets". In: *Journal of Mathematical Biology* 1 (1975), pp. 259–273.
[20] Antoni Guillamon and Gemma Huguet. "A computational and geometric approach to phase resetting curves and surfaces". In: *SIAM Journal on Applied Dynamical Systems* 8.3 (2009), pp. 1005–1042.
[21] Zhao-Zhe Hao et al. "Strong interactions between spinal cord networks for locomotion and scratching". In: *Journal of neurophysiology* 106.4 (2011), pp. 1766–1781.
[22] Michael Hardy. "Combinatorics of Partial Derivatives". In: *arXiv preprint math /0601149* (2006).
[23] Eugene M Izhikevich. *Dynamical Systems in Neuroscience*. MIT press, 2007.
[24] Akram Jafari Roodbandi, Alireza Choobineh, and Somayeh Daneshvar. "Relationship between circadian rhythm amplitude and stability with sleep quality and sleepiness among shift nurses and health care workers". In: *International Journal of Occupational Safety and Ergonomics* 21.3 (2015), pp. 312–317.
[25] Megan E Jewett, Daniel B Forger, and Richard E Kronauer. "Revised limit cycle oscillator model of human circadian pacemaker". In: *Journal of Biological Rhythms* 14.6 (1999), pp. 493–500.
[26] Peter C St John et al. "Amplitude metrics for cellular circadian bioluminescence reporters". In: *Biophysical Journal* 107.11 (2014), pp. 2712–2722.
[27] Dominic Jordan and Peter Smith. *Nonlinear ordinary differential equations: an introduction for scientists and engineers*. OUP Oxford, 2007.
[28] James P Keener. *Principles of Applied Mathematics: Transformation and Approximation*. CRC Press, 2018.

[29] István Z Kiss, Yumei Zhai, and John L Hudson. “Emerging coherence in a population of chemical oscillators”. In: *Science* 296.5573 (2002), pp. 1676–1678.

[30] Nikolai Mitrofanovich Krylov and Nikolai Nikolaevich Bogoliubov. *Introduction to Non-Linear Mechanics*. 11. Princeton University Press, 1950.

[31] Vincent Kulke et al. “A method for the design and optimization of nonlinear tuned damping concepts to mitigate self-excited drill string vibrations using multiple scales lindstedt-poincaré”. In: *Applied Sciences* 11.4 (2021), p. 1559.

[32] Yoshiki Kuramoto. *Chemical oscillations, waves, and turbulence*. Springer, 1984.

[33] Yueheng Lan and Igor Mezić. “Linearization in the large of nonlinear systems and Koopman operator spectrum”. In: *Physica D: Nonlinear Phenomena* 242.1 (2013), pp. 42–53.

[34] Benjamin Letson and Jonathan E Rubin. “A new frame for an old (phase) portrait: Finding rivers and other flow features in the plane”. In: *SIAM Journal on Applied Dynamical Systems* 17.4 (2018), pp. 2414–2445.

[35] Shijun Liao. *Beyond perturbation: introduction to the homotopy analysis method*. Chapman and Hall/CRC, 2003.

[36] Chengju Liu, Qijun Chen, and Jiaqi Zhang. “Coupled van der Pol oscillators utilised as central pattern generators for quadruped locomotion”. In: *2009 Chinese Control and Decision Conference*. IEEE. 2009, pp. 3677–3682.

[37] Jose-Luis Lopez, Saied Abbasbandy, and Ricardo Lopez-Ruiz. “Formulas for the amplitude of the van der Pol limit cycle through the homotopy analysis method”. In: *Scholarly Research Exchange* 2009 (2009).

[38] Lesley Ann Low et al. “Coupled van der Pol oscillators as a simplified model for generation of neural patterns for jellyfish locomotion”. In: *Structural Control and Health Monitoring: The Official Journal of the International Association for Structural Control and Monitoring and of the European Association for the Control of Structures* 13.1 (2006), pp. 417–429.

[39] David N Lyttle et al. “Robustness, flexibility, and sensitivity in a multifunctional motor control model”. In: *Biological cybernetics* 111 (2017), pp. 25–47.

[40] Joseph P McKenna et al. “Glucose oscillations can activate an endogenous oscillator in pancreatic islets”. In: *PLoS computational biology* 12.10 (2016), e1005143.

[41] Hil Gaétan Ellart Meijer and T Kalmár-Nagy. “The Hopf-van der Pol system: Failure of a homotopy method”. In: *Differential Equations and Dynamical Systems* 20 (2012), pp. 323–328.

[42] Ronald Mickens. “Comments on the method of harmonic balance”. In: *Journal of sound and vibration* 94.3 (1984), pp. 456–460.

[43] Bharat Monga et al. “Phase reduction and phase-based optimal control for biological systems: a tutorial”. In: *Biological Cybernetics* 113.1-2 (2019), pp. 11–46.

[44] Hiroya Nakao. “Phase reduction approach to synchronisation of nonlinear oscillators”. In: *Contemporary Physics* 57.2 (2016), pp. 188–214.

[45] Hinke M Osinga and Jeff Moehlis. “Continuation-based computation of global isochrons”. In: *SIAM Journal on Applied Dynamical Systems* 9.4 (2010), 1201–1228.

[46] Youngmin Park and Dan D Wilson. “High-order accuracy computation of coupling functions for strongly coupled oscillators”. In: *SIAM Journal on Applied Dynamical Systems* 20.3 (2021), pp. 1464–1484.

[47] Alberto Pérez-Cervera, Benjamin Lindner, and Peter J Thomas. “Isostables for stochastic oscillators”. In: *Physical Review Letters* 127.25 (2021), p. 254101.

[48] Alberto Pérez-Cervera, Benjamin Lindner, and Peter J Thomas. "Quantitative comparison of the mean–return-time phase and the stochastic asymptotic phase for noisy oscillators". In: *Biological Cybernetics* 116.2 (2022), pp. 219–234.
[49] Alberto Pérez-Cervera, Tere M-Seara, and Gemma Huguet. "Global phase-amplitude description of oscillatory dynamics via the parameterization method". In: *Chaos: An Interdisciplinary Journal of Nonlinear Science* 30.8 (2020), p. 083117.
[50] Alberto Pérez-Cervera et al. "A Universal Description of Stochastic Oscillators". In: *arXiv preprint arXiv:2303.03198* (2023).
[51] Hong Qi et al. "The Oscillation Amplitude, not the Frequency of Cytosolic Calcium, Regulates Apoptosis Induction". In: *iScience* 23.11 (2020), p. 101671.
[52] Wei Qiao, John T Wen, and Agung Julius. "Entrainment control of phase dynamics". In: *IEEE Transactions on Automatic Control* 62.1 (2016), pp. 445–450.
[53] Kevin Rompala, Richard Rand, and Howard Howland. "Dynamics of three coupled van der Pol oscillators with application to circadian rhythms". In: *Communications in Nonlinear Science and Numerical Simulation* 12.5 (2007), pp. 794–803.
[54] Reinhardt Mathias Rosenberg. "The normal modes of nonlinear n-degree-of-freedom systems". In: *Journal of Applied Mechanics* (1962).
[55] Angela M dos Santos, Sergio R Lopes, and RL Ricardo L Viana. "Rhythm synchronization and chaotic modulation of coupled Van der Pol oscillators in a model for the heartbeat". In: *Physica A: Statistical Mechanics and its Applications* 338.3-4 (2004), pp. 335–355.
[56] Cristina P Santos, Nuno Alves, and Juan C Moreno. "Biped locomotion control through a biomimetic CPG-based controller". In: *Journal of Intelligent & Robotic Systems* 85 (2017), pp. 47–70.
[57] Justus TC Schwabedal and Arkady Pikovsky. "Phase description of stochastic oscillations". In: *Physical Review Letters* 110.20 (2013), p. 204102.
[58] Steven W Shaw and Christophe Pierre. "Normal modes for non-linear vibratory systems". In: *Journal of Sound and Vibration* 164.1 (1993), pp. 85–124.
[59] Steven W Shaw and Christophe Pierre. "Normal modes of vibration for non-linear continuous systems". In: *Journal of Sound and Vibration* 169.3 (1994), pp. 319–347.
[60] Himanshu Shukla and Mayuresh Patil. "Control of limit cycle oscillation amplitudes in nonlinear aerelastic systems using nonlinear normal modes". In: *AIAA Atmospheric Flight Mechanics Conference*. 2016, p. 2004.
[61] Himanshu Shukla and Mayuresh J Patil. "Controlling limit cycle oscillation amplitudes in nonlinear aeroelastic systems". In: *Journal of Aircraft* 54.5 (2017), pp. 1921–1932.
[62] Eric Souêtre et al. "Circadian rhythms in depression and recovery: evidence for blunted amplitude as the main chronobiological abnormality". In: *Psychiatry Research* 28.3 (1989), pp. 263–278.
[63] Klaus M Stiefel and G Bard Ermentrout. "Neurons as oscillators". In: *Journal of Neurophysiology* 116.6 (2016), pp. 2950–2960.
[64] Steven H Strogatz. *Nonlinear dynamics and chaos: with applications to physics, biology, chemistry, and engineering*. CRC press, 2018.
[65] Annette F Taylor et al. "Dynamical quorum sensing and synchronization in large populations of chemical oscillators". In: *Science* 323.5914 (2009), pp. 614–617.

[66] Peter J Thomas and Benjamin Lindner. “Asymptotic phase for stochastic oscillators”. In: *Physical Review Letters* 113.25 (2014), p. 254101.

[67] Yangyang Wang et al. “Shape versus timing: linear responses of a limit cycle with hard boundaries under instantaneous and static perturbation”. In: *SIAM Journal on Applied Dynamical Systems* 20.2 (2021), pp. 701–744.

[68] Yangyang Wang et al. “Variational and phase response analysis for limit cycles with hard boundaries, with applications to neuromechanical control problems”. In: *Biological Cybernetics* 116.5-6 (2022), pp. 687–710.

[69] Zhelong Wang, Qin Gao, and Hongyu Zhao. “CPG-inspired locomotion control for a snake robot basing on nonlinear oscillators”. In: *Journal of Intelligent & Robotic Systems* 85 (2017), pp. 209–227.

[70] Kyle CA Wedgwood et al. “Phase-amplitude descriptions of neural oscillator models”. In: *The Journal of Mathematical Neuroscience* 3 (2013), pp. 1–22.

[71] Dan Wilson. “A direct method approach for data-driven inference of high accuracy adaptive phase-isostable reduced order models”. In: *Physica D: Nonlinear Phenomena* 446 (2023), p. 133675.

[72] Dan Wilson. “Phase-amplitude reduction far beyond the weakly perturbed paradigm”. In: *Physical Review E* 101.2 (2020), p. 022220.

[73] Dan Wilson and Bard Ermentrout. “Greater accuracy and broadened applicability of phase reduction using isostable coordinates”. In: *Journal of Mathematical Biology* 76 (2018), pp. 37–66.

[74] Dan Wilson and Bard Ermentrout. “Phase models beyond weak coupling”. In: *Physical Review Letters* 123.16 (2019), p. 164101.

[75] Dan Wilson and Jeff Moehlis. “Isostable reduction of periodic orbits”. In: *Physical Review E* 94.5 (2016), p. 052213.

[76] Arthur T Winfree. *The Geometry of Biological Time*. Vol. 2. Springer, 1980.

[77] Zhuojun Yu and Peter J Thomas. “A homeostasis criterion for limit cycle systems based on infinitesimal shape response curves”. In: *Journal of Mathematical Biology* 84.4 (2022), p. 24.

[78] Anatoly Zlotnik and Jr-Shin Li. “Optimal asymptotic entrainment of phase-reduced oscillators”. In: *Dynamic Systems and Control Conference*. Vol. 54754. 2011, pp. 479–484.